

Highlights

- Lignin fate in the hydrothermal conversion of giant reed to LA was studied.
- Hydrochar was characterized by Py-GC/MS, TGA/FTIR, and EGA-MS.
- Simple lignin derivatives were identified both in the liquid phase and hydrochar.
- Mother liquor and hydrochar washings were analyzed for antioxidant activity.
- Promising antioxidant properties were ascertained for the liquid fractions.
- This multi-valorisation improves the sustainability/economy of the LA process.

1 **Multi-valorisation of giant reed (*Arundo Donax* L.) to give levulinic acid**
2 **and valuable phenolic antioxidants**

3 Domenico Licursi¹, Claudia Antonetti¹, Marco Mattonai¹, Lorena Pérez-Armada², Sandra
4 Rivas², Erika Ribechini¹, Anna Maria Raspolli Galletti^{1*}

5 ¹ *Department of Chemistry and Industrial Chemistry, University of Pisa, Via G. Moruzzi 13, 56124,*
6 *Pisa, Italy.*

7 ² *Chemical Engineering Department, Polytechnical Building, University of Vigo (Campus Ourense), As*
8 *Lagoas, 32004, Ourense, Spain.*

9

10 *Corresponding author. *E-mail address:* anna.maria.raspolli.galletti@unipi.it

11

12 **Abstract**

13 Up to now, **on the industrial scale**, the acid-catalysed hydrothermal conversion of lignocellulosic biomass has
14 been targeted to the production of levulinic acid (LA), while the lignin fate has been neglected, **and its use has**
15 **been limited at most to the energy recovery**. Now, an integrated investigation of the hydrothermal process for the
16 synthesis of LA starting from giant reed (*Arundo Donax* L.) was studied taking into account the lignin phenol
17 derivatives present in the liquid phase and in the solid hydrochar. The analysis of the hydrochar was carried out
18 adopting coupled pyrolysis techniques, e.g. Py-GC/MS, TGA/FTIR, and EGA-MS, paying a special attention to
19 the contribution of the evolved simple phenolics. The hydrochar washing fractions were analyzed for the total
20 phenolic content (TPC) and antioxidant activity (AA), adopting TEAC, FRAP, and DPPH standard essays,
21 comparing the antioxidant activities with those deriving from the starting LA-rich mother liquor. Two washing
22 cycles allowed the complete recovery of the phenolic compounds of interest, leached from the porous hydrochar.
23 Also the starting LA-rich liquor was of great interest for the same purpose, having the highest content of these
24 compounds, which must be necessarily removed for the production of the commercial pure LA. Promising
25 antioxidant properties were ascertained for the mother liquor and the hydrochar washings, obtaining good linear
26 correlations between total phenolic compounds (TPC) and antioxidant capacity (TEAC, FRAP, and DPPH). This

27 multi-valorisation approach contributes to improving the sustainability of the entire LA process and shifts the
28 attention towards the antioxidants, new niche bioproducts of great interest, which add significant economic value
29 to the overall Biorefinery of the lignocellulosic biomass.

30

31 **Keywords:** levulinic acid; lignin; hydrochar; water-soluble phenolics; antioxidants; giant reed.

32

33 **1. Introduction**

34 The acid-catalyzed hydrothermal route is one of the most promising and environmentally friendly processes for
35 biomass exploitation (Jin et al., 2014). Nowadays, this process is mostly addressed to the production of levulinic
36 acid (LA), the C5 ketocarboxylic acid which is considered as one of the top bio-based platform molecules of
37 greatest industrial interest, thanks to its feasible upgrading into other bio-products, including solvents,
38 plasticizers, fuels and oxygenated fuel additives, monomers for polymers, etc. (Antonetti et al., 2016; Freitas et
39 al., 2016; Pileidis and Titirici, 2016; Rivas et al., 2016). The mature industrial technologies for LA synthesis are
40 based on the exploitation of biomasses rich in C6 or C5 sugars, which are converted through the respective
41 different conversion mechanisms (Van der Waal and De Jong, 2016). Regarding the C6 conversion pathway,
42 LA formation proceeds by acid-catalysed hydrolysis/dehydration, which gives 5-hydroxymethylfurfural (5-HMF)
43 as intermediate (Mukherjee et al., 2015). This furanic compound can be selectively produced, under appropriate
44 reaction conditions (Antonetti et al., 2017a, 2017b), being itself a versatile molecule, which can be further
45 transformed into added-value biofuels and bioproducts. Harsher reaction conditions, in term of acidity, reaction
46 temperature and time, allow the fast transformation of the 5-HMF intermediate into LA, therefore including an
47 additional rehydration step (Antonetti et al., 2016). The technology of the LA process based on the C6 route has
48 been developed by Biofine Renewables (Hayes et al., 2006) and updated by GFBiochemicals (2017), which has
49 recently announced new plans to expand its production on a commercial scale (Silva et al., 2017). During the C6
50 conversion route, any pentoses of the same lignocellulosic feedstock are converted into furfural (FUR), another
51 very valuable platform chemical (Bernal et al., 2014). This furanic intermediate could be continuously isolated
52 introducing a milder preliminary hydrolysis step (Parton et al., 2013), but actually it is not recovered within the
53 process, remaining in the same reaction medium, where it degrades almost completely, under the harsher
54 reaction conditions suitable for LA synthesis (Antonetti et al., 2015). The main degradation by-products of the

55 C5/C6 sugar conversion are called “humins”, which derive from condensation reactions involving furanic
56 intermediates (e.g. FUR and 5-HMF from C5 and C6 conversion, respectively) and precursor sugars (e.g. mainly
57 glucose and xylose), with precipitation of an insoluble carbonaceous solid (Heltzel et al., 2016; Tsilomelekis et
58 al., 2016; Wang et al., 2016). Heltzel et al. (2016) have confirmed that the synthesis of huminic by-products
59 involves polymerization of simple furanics, via an aldol addition/condensation pathway. In particular, the authors
60 have studied in depth the thermodynamics of humin formation, suggesting that, taking into account the
61 hydrolysis of C6-sugars, the ring opening of the 5-hydroxymethylfurfural (5-HMF) leads to the main formation of
62 2,5-dioxo-6-hydroxyhexanal, which undergoes further aldol addition/condensation, resulting, in this way, the
63 primary building block of these furanic by-products. Although not yet unequivocally determined, the humin
64 structure is known to depend on the reaction temperature, time, acid concentration, feedstock structure and its
65 concentration (Zandvoort et al., 2013; Antonetti et al., 2017a). All these parameters must be carefully optimized
66 for the selective synthesis of LA but, unfortunately, humins are always formed under the best LA reaction
67 conditions. In our specific case, starting from C6-sugars, the 5-HMF intermediate is not detected under the best-
68 adopted reaction conditions for LA synthesis, thus highlighting its complete conversion to both LA and humins.
69 About 40 wt% yields of humins were reported in the mineral acid dehydration of aldose, while yields up to 50
70 wt% of huminic by-products can derive from 5-HMF production (Filiciotto et al., 2017). In addition, humins may
71 derive also from C5 (hemicellulose) degradation reactions, involving furfural formation as the main intermediate,
72 which is no more present, also in this case, under the best reaction conditions for LA synthesis, further
73 confirming its degradation into humins (Licursi et al., 2015). Summerskii et al. (2010) studied the multi-step humin
74 formation in acidic medium from monosaccharides, underlining that C5-sugars yielded more humins than the C6-
75 ones. This result was ascribed to the higher reactivity of furfural, readily formed from C5 sugars, which
76 undergoes further condensation reactions to humins, whereas lower thermal stability caused the decomposition
77 of 5-HMF into LA and FA. In fact, kinetic studies on humin formation have reported values of activation energies
78 in the range 85-130 kJ mol⁻¹ for humin formation from 5-HMF, whereas lower activation energies were found for
79 the humins formed from furfural (Filiciotto et al., 2017). Regarding the lignin fraction, on the basis of the available
80 optimized LA technology, the isolation of lignin upstream still remains not economically advantageous, adding
81 significant separation costs to the entire LA process. Therefore, lignin is recovered downstream and partially
82 burnt for energy recovery within the same LA plant, otherwise, the remaining stream is currently disposed of. As
83 a consequence, all the new exploitation strategies of lignin fraction recovered after LA production are well-

84 appreciated, adding further economic value to the entire LA process. Regarding the lignin chemistry during the
85 acid hydrothermal treatment, the combined effect of acidity, temperature and residence time allows the breaking
86 of the more labile ether bonds between its units, leading to its partial fragmentation, but, unfortunately, their fast
87 condensation prevails, resulting in the formation of more stable C-C bonds (Kang et al., 2013; Wang et al., 2013;
88 Zhang et al., 2015). Furthermore, appropriate reaction conditions for lignin dissolution and hydrolysis to
89 monomers by the hydrothermal route are significantly harsher than those adopted for LA synthesis, requiring the
90 use of near-critical or supercritical water (Pavlovič et al., 2013). The native lignin fraction undergoes a
91 degradation, becoming a “pseudo-lignin” (Zhuang et al., 2017), which may condense with humins forming the
92 final solid “hydrochar”, which is directly separated from the LA-rich mother liquor by simple filtration (Licursi et al.,
93 2017). Thanks to its improved energetic properties, hydrochar can be directly burnt within the same LA plant,
94 thus partially recovering the energy of the entire process but, due to the abundance of this waste stream, which
95 strongly depends on the lignin content of the starting feedstocks, it is necessary to find new exploitation
96 possibilities, thus ensuring the best circular economy approach. In this context, another different exploitation
97 possibility of this hydrochar has been reported by Bernardini et al. (2017), who investigated the synthesis of
98 flexible polyurethane foams by lignin liquefaction in polyolic solvents under microwave irradiation. For different
99 purposes, the entire biomass can be liquefied under relatively mild conditions using polyalcohols, being this step
100 mandatory for subsequent upgrading step, such as its hydrotreatment for the production of oils (Grilc et al.,
101 2014a, 2014b, 2015).

102 Giant reed (*Arundo Donax* L.) represents a well-known promising feedstock for LA production (Antonetti et al.,
103 2015), due to its rapid growth rate, high resource-use efficiency (of water, radiation, and nutrients), good
104 tolerance to biotic (pests and diseases) and abiotic (heat, freezing, salts) stress and high productivity (Bosco et
105 al., 2016). Furthermore, it represents a very good source of lignin (~20-25 wt%, as Klason lignin), which is
106 composed of *p*-hydroxyphenyl (H), guaiacyl (G), and syringyl (S) phenylpropanoid units, bonded with a
107 predominance of β -O-4' aryl ether linkages (~70-80 %), with the remaining part constituted by β - β' , β -5', β -1',
108 and α,β -diaryl ether linkages (You et al., 2013). Gas Chromatography/Mass Spectrometry (GC/MS) technique
109 was adopted to characterize both qualitatively and quantitatively the monosaccharide composition of the starting
110 *Arundo Donax* L., whilst analytical pyrolysis (Py-GC/MS) was used to characterize the starting biomass and the
111 hydrochars recovered after FUR and LA production, thus monitoring the progress of the C5/C6 hydrothermal
112 conversion (Ribechini et al., 2012). It was demonstrated that Py-GC/MS was a powerful tool for monitoring the

113 chemical modification of the biomass during its catalytic conversion. It was found that, despite the occurred
114 degradation of the lignin, it was still possible to detect simple low-molecular phenols. The solid hydrochar shows
115 a “lignite-like” behavior, which corresponds to very interesting energetic properties (Licursi et al., 2015).
116 Furthermore, this solid waste is rich in carbonyl and hydroxyl reactive functionalities, which make it sustainable
117 for many other applications in environmental, catalysis and polymer chemistry. In particular, a novel green
118 synthesis of flexible polyurethane foams, adopting the *Arundo Donax* L. hydrochar as pseudo-lignin polyol
119 source, has been recently reported (Bernardini et al., 2017).

120 While the fate of the solid phase deriving from the hydrothermal process has been mostly defined by the
121 characterization activity, little is known about the composition of the phenolic fraction contained in the water
122 phase. This aspect is of paramount importance for closing the Biorefinery of the different hydrothermal
123 processes, thus justifying their complete circular economy (Jin and Enomoto, 2011). For example, Savy et al.
124 (2015a) have investigated the molecular composition of water-soluble lignins obtained after alkaline oxidation
125 treatment of miscanthus (*Miscanthus x Giganteus, Greef et Deuter*) and giant reed (*Arundo Donax* L.). The
126 authors have found that guaiacyl units were the main water-soluble units, followed by syringyl subunits, and few
127 condensed fragments. Low carbohydrate content indicated that alkaline oxidation efficiently separated water-
128 soluble lignin from lignocellulose. In subsequent investigations, the same authors (Savy et al., 2015b, 2016)
129 have proposed the use of these water-soluble lignins as plant biostimulants for the germination and early growth
130 of maize (*Zea mays, L.*) seedlings. Furthermore, the recovery of phenolic compounds from hydrolysates has
131 been mostly investigated after milder pretreatments, as in the case of the pre-hydrolysis of yellow poplar by
132 oxalic acid (Um et al., 2017), whilst, at this state of the art, the opportunity of recovering the phenolic compounds
133 downstream of LA production has not been proposed. In this paper, the study of the lignin behavior during the
134 acid-catalysed hydrothermal conversion of *Arundo Donax* L. to LA has been investigated in-depth, taking into
135 account both solid and liquid phase and the antioxidant activity of the obtained phenolics has been evaluated,
136 thus demonstrating this new exploitation possibility for a multi-valorization of the starting biomass.

137

138 **2. Materials and methods**

139 **2.1. Materials**

140 Giant reed (*Arundo Donax* L.) was provided by the Institute of Life Sciences Scuola Superiore Sant'Anna of
141 Pisa. It came from long-term field trials carried out in Central Italy at the Enrico Avanzi Interdepartmental Centre
142 for Agro-Environmental Research (CIRAA) of the University of Pisa, located in San Piero a Grado (PI) (latitude
143 43° 68' N, longitude 10° 35' E). The raw biomass was dried at 60 °C in a thermo-ventilated oven until a constant
144 weight was reached and it was stored in a desiccator up to its use. The composition of the **whole** starting
145 biomass (**stalks/leave ratio = 70/30**) was the following: 65.3 wt% structural polysaccharides (25.8 wt%
146 hemicellulose and 39.5 wt% cellulose), 26.1 wt% lignin (24.3 wt% as Klason lignin + 1.8 wt% as acid-soluble
147 lignin), 4.2 wt% extractives and 4.4 wt% ash (Licursi et al., 2015).

148 Hexamethyldisilazane (HMDS) and N,O-bis(trimethylsilyl)trifluoroacetamide (BSTFA) with or without 1%
149 trimethylchlorosilane (TMCS) were purchased from Sigma-Aldrich (Milan, Italy). Tridecanoic acid, hexadecane
150 were purchased from Sigma–Aldrich (USA). All the adopted solvents were HPLC grade.

151

152 **2.2. Hydrolysis reactions**

153 Hydrolysis reactions were carried out both in the microwave and in autoclave reactors. Regarding the first
154 system, the reactions were carried out by using a commercially available mono-mode microwave reactor (CEM
155 Discover S-Class System, NC, USA), adopting a 35 mL vessel containing a teflon stir bar. This system was
156 equipped with a built-in keypad for programming the reaction procedures and allowing on-the-fly changes. The
157 adopted output power was 300 W, sufficient for rapid heating of the aqueous slurry. Temperature measurement
158 during the reaction was achieved by an IR sensor positioned at the bottom of the cavity, below the vessel. **Water**
159 **and HCl (1.66% wt) were mixed with biomass in a liquid to solid ratio (LSR) of 15 g/g**, and introduced into the
160 vessel, then it was closed and irradiated up to the set-point temperature (190 °C), by employing a fixed ramping
161 time, and maintained at this temperature for 20 minutes. At the end of the reaction, the reactor was rapidly
162 cooled up to room temperature by means of air which was blown directly on the surface of the reactor. The
163 reaction mixture was filtered on a Büchner filter and the mother liquor was analyzed by HPLC for the
164 quantification of the LA and by GC/MS for the identification of phenolic compounds. Instead, the hydrochar was

165 washed with 50 mL of fresh water, then dried at 105 °C for 24 h and stored in a desiccator up to its next
166 characterization.

167 Then, the hydrolysis reaction was scaled up in a 1 L Hastelloy C autoclave (Renato Brignole Instruments). The
168 autoclave was equipped with a mechanical magnetic stirrer system, a heating system consisting of three ceramic
169 resistors (each of 500 W) and a thermocouple sensor for monitoring the temperature inside the autoclave. The
170 process control was a Poly Dispersity Index (P.D.I.) and was based on the measurement of the absorbed
171 electrical current by the three resistors. The same solid to liquid weight ratio of the MW tests was adopted.
172 Therefore, water and HCl were mixed with biomass in the same concentration (1.66% wt) and LSR (15 g/g),
173 already adopted for the experiments carried out in microwave (see above). The mixture was introduced into the
174 autoclave and then it was closed and pressurized with 20 bars of nitrogen, heated to the reaction temperature
175 (190 °C) and maintained at this temperature for 1 h. At the end of each hydrolysis reaction, the autoclave was
176 cooled down to room temperature by means of water, which was flown into the jacket and then degassed. The
177 reaction mixture was recovered and filtered on a Buchner filter, then the mother liquor was analyzed for the
178 identification of the phenolic compounds, for the quantification of LA, total phenolic content and antioxidant
179 activity. Instead, the recovered wet *Arundo Donax* L. hydrochar (~18.5 g) was directly washed on the Büchner
180 filter four times (each time adopting 250 mL of fresh water), dried at 105 °C for 24 h and stored in a desiccator
181 up to its next characterization. Each washing fraction was separately recovered and further characterized for the
182 identification of the phenolic compounds and the determination of the antioxidant activity and the total phenolic
183 content.

184

185 **2.3. Quantitative analysis of the mother liquor and hydrochar**

186 The quantitative analysis of the mother liquor was performed by High Performance Liquid Chromatography
187 (HPLC). For this purpose, a Perkin Elmer Flexar Isocratic Platform, which was equipped with a differential
188 refractive index detector, was used. 20 µL samples were loaded into a column Benson 2000-0 BP-OA (300 mm
189 × 7.8 mm) kept at 60 °C, employing 0.005 M H₂SO₄ as a mobile phase (flow rate, 0.6 mL min⁻¹). The calibration
190 was carried out using a commercial standard of LA. At least three replicates for each concentration of LA
191 standard were carried out. The reproducibility of the technique was within 2%.

192 The mass yield of the LA was calculated as follows:

193

194
$$LA \text{ mass yield (wt\%)} = [\text{mass of LA in the reaction mixture (g)}/\text{raw material (g)}] \times 100 \quad (1)$$

195

196 The yield of LA based on theoretical yield was calculated taking into account the stoichiometry of the reaction
197 involving the co-formation of formic acid starting from cellulose.

198

199
$$\% \text{ on theoretical LA yield} = [\text{LA in the reaction mixture (g)}/(\text{raw material (g)} \times \text{cellulose content} \times 0.7155)] \times 100$$

200 (2)

201

202 Lastly, the mass yield of the recovered hydrochar was calculated as follows:

203

204
$$\text{Hydrochar yield (wt\%)} = [\text{dried hydrochar (g)}/\text{raw material (g)}] \times 100 \quad (3)$$

205

206 **2.4. Pyrolysis-Gas Chromatography/Mass Spectrometry (Py-GC/MS) of the microwave- and** 207 **autoclave- derived *Arundo Donax* L. hydrochars**

208 Pyrolysis/Gas Chromatography/Mass Spectrometry (Py-GC/MS) was used to investigate the chemical
209 composition of the hydrochars recovered after hydrothermal treatment of *Arundo Donax* L. for LA production,
210 adopting traditional and microwave heating. All the solid samples were dried in an oven at 60 °C for 15 h and
211 milled before the Py-GC/MS analysis. The used ball mill was Mini-Mill PULVERISETTE 23, with grinding bowls
212 (15 mL) and grinding balls (0.5 mm) made of zirconium oxide. Py-GC/MS analysis was carried out using an
213 EGA/PY-3030D Multi-Shot micro-furnace pyrolyser (Frontier Lab, Japan). The pyrolysis temperature was 550°C
214 and interface temperature was 250 °C. Similar amounts (ca. 100 µg) of the sample and HMDS (5 µL) were put
215 into a stainless steel cup and placed into the micro-furnace. The GC injector was used with a split ratio of 1:10
216 and 280 °C. Chromatographic conditions were as follows: initial temperature 50 °C, 1 min isothermal, 10 °C min⁻¹
217 to 100 °C, 2 min. isothermal, 4 °C min⁻¹ to 190 °C, 1 min. isothermal, 30 °C min⁻¹ to 280 °C, 30 min. isothermal.
218 Carrier gas: Helium (purity 99.995%), constant flow 1.0 mL min⁻¹. The pyrolyzer was connected to a gas
219 chromatograph 6890 Agilent (USA) equipped with a split/splitless injector, an HP-5MS fused silica capillary
220 column (stationary phase 5% diphenyl- and 95% dimethyl-polysiloxane, 30 m x 0.25 mm i.d., Hewlett Packard,
221 USA) and with a deactivated silica pre-column (2 m x 0.32 mm i.d., Agilent J&W, USA). The GC was coupled

222 with an Agilent 5973 Mass Selective Detector operating in electron impact mode (EI) at 70 eV. The MS transfer
223 line temperature was 300 °C. The MS ion source temperature was kept at 230 °C and the MS quadrupole
224 temperature at 150 °C. Peak areas of the pyrolysis products were measured, and the data for three replicated
225 analyses averaged and expressed as normalized percentages. The relative standard deviation for the relative
226 areas of the peaks was between 5 and 10%.

227

228 **2.5. Thermogravimetric analysis/Infrared Spectroscopy (TGA/FTIR) of the microwave- and** 229 **autoclave-derived *Arundo Donax* L. hydrochars**

230 Thermogravimetric analysis (TGA) was performed by a TGA-DSC 1LF/164 (Mettler Toledo) in high purity N₂ at a
231 flow rate of 60 mL/min. The thermogravimetric balance was coupled with an analyzer FTIR NEXUS (Thermo
232 Fisher Scientific) for the analysis of the evolved volatiles. The sample (~10 mg) was heated from 30 °C up to 900
233 °C, at a rate of 10 °C min⁻¹, under a nitrogen atmosphere (60 ml min⁻¹). Each FT-IR spectrum was acquired
234 every 32 seconds, resulting in 163 acquired spectra in total, for any experiment. TGA and FTIR were connected
235 by a heated transfer line with a temperature of 220 °C for preventing the condensation of gaseous products.
236 FTIR spectra were acquired in the range 4000-400 cm⁻¹, by using the OMNIC software. Both TG (weight loss as
237 a function of temperature) and DTG (rate of mass loss as a function of the temperature increase) curves were
238 acquired during each experiment. The identification of the FTIR spectra of the hydrochar was carried out on the
239 basis of the available electronic libraries. Each test was carried out in duplicate in order to verify the
240 reproducibility and accuracy of the experimental data.

241

242 **2.6. Evolved Gas Analysis coupled with Mass Spectrometry (EGA-MS) of the microwave- and** 243 **autoclave- derived *Arundo Donax* L. hydrochars**

244 Evolved gas analysis-mass spectrometry (EGA-MS) of the starting *Arundo Donax* L. and its hydrochars was
245 carried out using a micro-furnace pyrolyser (Multi-Shot EGA/PY-3030D Pyrolyzer, Frontier Lab) directly coupled
246 with a 5973 Mass Selective Detector (Agilent Technologies, Palo Alto, CA, USA) single quadrupole mass
247 spectrometer via a deactivated and uncoated stainless steel transfer tube (UADTM-2.5N, 0.15 mm i.d. × 2.5 m
248 length, Frontier Lab). About 0.2-0.4 mg of sample were adopted for each experiment and placed into a steel
249 sample cup. The temperature of the micro-furnace pyrolyzer was programmed from 50 °C to 700 °C, at a

250 heating rate of 12 °C min⁻¹, under a helium flow (1 mL min⁻¹), with a split ratio 1:50. The micro-furnace interface
251 temperature was kept at 320 °C and the temperature of the oven was maintained isothermally at 300 °C. The
252 mass spectrometer was operated in EI positive mode (70 eV, scanning m/z 50-600). The MS transfer line
253 temperature was 300 °C. The MS ion source temperature was kept at 230 °C and that of the MS quadrupole at
254 150 °C.

255

256 **2.7. Gas Chromatography/Mass Spectrometry (GC/MS) of the mother liquor and hydrochar** 257 **washings**

258 GC/MS was used to study the composition of the starting liquor derived from *Arundo Donax* L. hydrolysis and
259 hydrochar washings. 1 mL of the starting liquor and each washing were acidified with 1 mL of HCl 6M and then
260 extracted with diethyl ether (600 µL, three times), dried under nitrogen flow and re-dissolved with 1mL of Et₂O.
261 200 µL of the obtained organic phase were dried under nitrogen flow and derivatized for GC/MS analysis, adding
262 5 µL of internal standard (tridecanoic acid in acetone) and 20 µL of derivatizing agent N,O-
263 bis(trimethylsilyl)trifluoroacetamide (BSTFA). The reaction took place at 60 °C for 30 minutes in 150 µL of
264 isooctane. 10 µL of the injection internal standard (hexadecane in isooctane) were added before injection in
265 GC/MS (2 µL).

266 Chromatographic separation was performed with a chemically bonded fused-silica capillary column HP-5MS
267 (Agilent Technologies, Palo Alto, CA, USA), stationary phase 5% phenyl–95% methylpolysiloxane, 0.25 mm
268 internal diameter, 0.25 µm film thickness, 30 m length, connected to 2 m × 0.32 mm internal diameter
269 deactivated fused silica pre-column. The carrier gas was helium (99.995% purity) at a constant flow of 1.2
270 mL/min. The chromatographic conditions for the separation of silylated compounds were as follows: starting
271 temperature 80 °C, isothermal for 2 min, 10 °C/min. up to 200 °C, 200 °C, isothermal for 3 min, 10 °C min⁻¹ up to
272 280 °C, 280 °C, isothermal for 3 min., 20 °C/min. up to 300 °C, 300 °C, isothermal for 20 min. Chromatograms
273 were recorded in TIC (Total Ion Current, mass range 50–600).

274 6890N GC system gas chromatograph (Agilent Technologies) coupled with a 5975 mass selective detector
275 (Agilent Technologies) single quadrupole mass spectrometer and equipped with PTV injector, were used. The
276 mass spectrometer was operated in the EI positive mode (70 eV). The MS transfer line temperature was 280 °C,
277 the MS ion source temperature was kept at 230 °C, and the MS quadrupole temperature was kept at 150 °C.

278 The four fractions recovered from the washing of the autoclave-derived hydrochar were analyzed by the same
279 gas chromatographic method. To obtain an estimation of the recovery efficiency, all the chromatographic peaks
280 belonging to identified phenols were integrated and a total chromatogram area was calculated for each fraction.
281 Recovery efficiency (%) after n extractions, R_n , was then estimated with the formula $R_n = (1 - A_n/A_0) \times 100$,
282 where A_n is the total area of the n-th chromatogram, and A_0 is the area of the starting liquor.
283

284 **2.8. Content of soluble compounds in the mother liquor and water soluble fractions recovered** 285 **from hydrochar washings**

286 The content of soluble compounds (SC) was obtained and expressed on the basis of the content of non-volatile
287 compounds in the liquid phases. The content of non-volatile compounds (NVC) in the autoclave-derived mother
288 liquor and hydrochar washings was measured by oven-drying at 105 °C until constant weight (Sluiter et al.,
289 2008). The analyses were made in triplicate.
290

291 **2.9. Total phenolic content (TPC) of the mother liquor and hydrochar washings**

292 TPC of the autoclave-derived mother liquor and hydrochar washings was determined by the Folin-Ciocalteu
293 assay and expressed as gallic acid equivalents (GAE) (Singleton and Rossi, 1965). In addition, water-soluble
294 phenolics in the mother liquor were also measured by UV-Vis spectroscopy, as already done for the NREL
295 method used in our previous work for the characterization of the starting biomass (Licursi et al., 2015).
296

297 **2.10. Antioxidant activity (AA) of the mother liquor and hydrochar washings**

298 The Trolox Equivalent Antioxidant Capacity (TEAC) assay is based on the scavenging capacity against the
299 ABTS radical (2,20-azinobis-(3-ethyl-benzothiazoline-6-sulfonate)), converting it into a colorless product (Re et
300 al., 1999). The ability to reduce the ferric 2,4,6-tripyridyl-s-triazine (TPTZ) complex under acidic conditions was
301 determined by the FRAP assay (Benzie and Strain, 1996). The scavenging capacity against α,α -diphenyl- β -
302 picrylhydrazyl (DPPH) radical scavenging was determined according to Conde et al. (2008). The inhibition
303 percentage (%IP) of the DPPH radical was calculated as the percent of absorbance reduction after 16 min with
304 respect to the initial value. All the analysis were made in triplicate.
305

306 **3. Results and discussion**

307 **3.1. Synthesis of LA and hydrochar**

308 The *Arundo Donax* L. hydrolysis reactions to give LA and hydrochar were carried out starting from the
309 formulation and the reaction conditions which were previously optimized both in microwave and autoclave
310 systems (Antonetti et al., 2015; Licursi et al., 2015). **The optimized results for the synthesis of LA and hydrochar**
311 **are reported in Table 1, for the two different heating systems:**

312

313 Table 1, near here

314

315 The above data confirm the similarity of the LA and hydrochar mass yields obtained from the two different
316 heating systems. Different reaction times were necessary for achieving a complete conversion of the hexoses,
317 with a theoretical LA yield of ~75-78 %, evaluated respect to the cellulose content of the starting biomass and
318 the stoichiometry of the reaction, in agreement with our previous researches (Antonetti et al., 2015; Licursi et al.,
319 2015). Furthermore, the obtained results highlight that the hydrochar represents the main by-product of the LA
320 synthesis, approaching the mass yield of ~29-30 wt%, evaluated respect to the weight of the starting biomass,
321 and this high yield makes necessary its complementary exploitation. The chemical characterization of the
322 hydrochars synthesized by the two different heating systems is discussed in the next paragraphs.

323

324 **3.2. Lignin in the solid phase: Py-GC/MS of the microwave- and autoclave- derived *Arundo*** 325 ***Donax* L. hydrochars**

326 Table 2 lists the compounds identified in the pyrograms **of the hydrochars obtained by microwave- and**
327 **autoclave- hydrothermal treatment of *Arundo Donax* L. biomass.** The identification of the pyrolysis products has
328 been done on the basis of previous works (Mattonai et al., 2016; Ribechini et al., 2012).

329

330 Table 2, near here

331

332 The **data (Table 2 and Fig. S1 in supplementary material) show** that the two hydrochars have a similar pattern of
333 the evolved phenolic compounds, thus confirming the similarity between the two hydrolysis reactions. The

334 pyrolysis products of lignin source include mainly simple phenols, such as guaiacol, methyl guaiacol, ethyl
335 guaiacol, vinyl guaiacol, methyl syringol, vinyl syringol (Wang and Luo, 2017), all with high abundance, deriving
336 from lignin cleavage. On the other hand, Z-coniferyl alcohol, E-coniferyl alcohol, Z-sinapyl alcohol and E-sinapyl
337 alcohol, which were abundant pyrolysis products of the lignin fraction in the starting *Arundo Donax* L., showed
338 low abundance in both hydrochars. This result is related to the performed hydrothermal treatment, which has led
339 to the modification/degradation of the lignin side chains. The most interesting difference in the pyrolysate
340 composition of the two hydrochars regards mainly the presence of oxidized compounds, such as 2-
341 hydroxypropanoic acid (#2), butanedioic acid (#13), vanillin (#26), syringaldehyde (#36), and vanillic acid (#38),
342 which are present in greater percentages in the autoclave-derived hydrochar. This is due to the combined effect
343 of longer reaction time and the difficulty to guarantee a totally inert atmosphere in the autoclave reactor. In
344 addition, the pyrolysis products of cellulose and hemicellulose source have not been found, thus demonstrating
345 the complete conversion of the holocellulosic fraction. Finally, it is interesting to note that the evolved aromatic
346 compounds could be advantageously condensed as bio-oil, and therefore their further fractionation and
347 exploitation is highly desired, thus completing the biomass fractionation (Wang and Cheng, 2014).

348

349 **3.3. Lignin in the solid phase: TGA/FTIR and EGA-MS of the microwave- and autoclave-derived** 350 ***Arundo Donax* L. hydrochars**

351 Thermal behavior of the microwave- and autoclave- derived *Arundo Donax* L. hydrochars was compared with
352 that of the starting biomass. The thermogravimetric analysis represents a very quick and useful tool for
353 visualizing the changes in chemical composition (cellulose, hemicelluloses and lignin) occurred between the
354 starting biomass and the obtained hydrochar, depending on the employed reaction conditions. In fact, starting
355 *Arundo Donax* L. biomass has its own unmodified cellulose, hemicellulose, and lignin, whilst its derived
356 hydrochars include both degraded lignin and humins. The comparison between the TG/DTG profile of the starting
357 *Arundo Donax* L. biomass and those of the microwave- and autoclave-derived hydrochars is reported in Fig. 1:

358

359

Fig. 1, near here

360

361 The above figure confirms the analogous thermal profile of both *Arundo Donax* L. hydrochars, but these are very
362 different respect to that of the starting biomass. In detail, DTG curve of the starting biomass shows two intense
363 subsequent degradation steps between 200 and 400 °C, due to the progressive degradation of the hemicellulose
364 and cellulose fractions, respectively. Regarding the thermal behavior of the native lignin, its degradation cannot
365 be significantly appreciated by DTG, being very slow through a wide temperature range (100-800 °C), showing
366 only a weak derivative signal, which falls within those of the carbohydrates (Watkins et al, 2015). Instead, DTG
367 curves of the microwave- and autoclave- derived hydrochars highlight the absence of the thermal degradation
368 steps of hemicellulose/cellulose source, thus revealing the presence of the lignin fraction, which shows a
369 maximum degradation temperature at about 400 °C in both cases. This temperature is higher than that of the
370 native lignin fraction, thus demonstrating the improved thermal stability of the synthesized hydrochars. This is
371 further confirmed by considering the amount of the residual biochar in the TG curves, which is much more higher
372 for both hydrochars rather than for the starting biomass, at each temperature exceeding 500 °C. By coupling
373 TGA with FTIR, the type and distribution of the gaseous products can be linked to the weight loss stages during
374 the hydrochar pyrolysis process. The FTIR identifications of the gaseous compounds deriving from hydrochar
375 pyrolysis at 400 and 850 °C are reported as supplementary materials (Fig. S2 and Fig. S3 in supplementary
376 material), taking into account both the best-matched reference compounds and the available literature data (Yao
377 et al., 2017). Also the Gram-Schmidt plot, which defines the gas emission as a function of the time, is reported
378 as supplementary material in Fig. S4.
379 3D FTIR spectra of the pyrolysis gaseous products of autoclave-derived hydrochar are reported in Fig. 2, as a
380 clarification of the following discussion:

381
382 Fig. 2, near here
383

384 FTIR analysis of the gas deriving from hydrochar pyrolysis has revealed the prevailing presence of carbon
385 dioxide and, to a lesser extent, carbon monoxide, both throughout a wide temperature range, e.g. ~150-700 °C
386 and ~300-700 °C, respectively. Furthermore, the presence of methane (~300-800 °C), methanol (~250-550 °C)
387 and acetic acid (~220-750 °C) was also ascertained. Regarding the aromatic compounds, their distinctive
388 absorption bands have not been detected by FTIR, these being minor compounds, not detectable due to the
389 lower sensibility of this technique. In order to get more information about the chemical composition of the

390 evolved volatiles, with a particular attention to the aromatics, EGA-MS analysis of the same samples was carried
391 out. Thermograms of the gaseous phase evolved during the thermal degradation of the starting *Arundo Donax* L.
392 biomass and its microwave- and autoclave- derived hydrochars are reported in Fig. 3:

393

394

Fig. 3, near here

395

396 The above thermal profiles retrace mostly those obtained by the traditional TGA analysis (Fig. 1). The EGA-MS
397 profile of the starting *Arundo Donax* L. biomass shows only one main peak at about 330°C. In addition, a
398 shoulder is detected at a higher temperature (380-470°C). The mass spectra highlight that the first step was due
399 to the thermal degradation of both cellulose and lignin, because the relative mass spectrum (Fig. 4, a) contains
400 peaks of carbohydrate (m/z 60, 85, 98, 114,126) and lignin (m/z 137, 167, 180, 194, 208) source (Ribechini et
401 al., 2015; Tamburini et al., 2015). The mass spectra (Fig. 4, b) of the second degradation region (380-470 °C)
402 highlight the presence of the fragments at m/z 77 (benzenes), 91 (alkylbenzenes), 107 (alkylphenols) and 123
403 (alkylcatechols), among those most abundant. Such peaks are indicative of secondary pyrolysis products due to
404 secondary reactions involving demethylation and demethoxylation of guaiacyl and syringyl units, which occur at
405 high temperatures (Tamburini et al., 2015).

406

407

Fig. 4, near here

408

409 The *Arundo Donax* L. hydrochars show a very different EGA-MS profile (clearly respect to the starting untreated
410 biomass), both having only one degradation peak between 320 and 540 °C (Fig. 3). This different behavior is
411 due to remarkable differences in chemical composition and thermochemical stability of the analyzed samples. In
412 fact, the acquired data indicate that the hydrochars contain compounds which are more thermally stable, which
413 degrade at higher temperatures than those of the untreated biomass. In addition, the acquired mass spectra
414 within the entire time range (10-43 min, reported in Fig. 5), demonstrate that both hydrochars are pseudo-lignin
415 samples. In detail, the main peaks at m/z 77, 91, 107 and 123, come from lignin pyrolysis reactions to give
416 alkylbenzenes, alkylphenols, and alkylcatechols, involving demethylation and demethoxylation pathways. At the
417 same time, the occurrence of the peaks at m/z 151 and 181, which were produced by all the *p*-substituted

418 guaiacyl and syringyl units bearing a carbonyl group at the benzylic position, demonstrate that oxidation pathway
419 has occurred during both hydrothermal treatments (Tamburini et al., 2015).

420

421 [Fig. 5, near here](#)

422

423 **3.4. Lignin in the liquid phase: GC/MS of the mother liquor and hydrochar washings**

424 The mother liquors which were directly obtained by *Arundo Donax* L. hydrolysis under traditional and microwave
425 heating were further analyzed by GC/MS, [in order to evaluate the presence of lignin-source phenols derived](#)
426 [from the acid-catalysed hydrothermal treatment of the biomass. Moreover, this analysis is useful for revealing](#)
427 the possible differences caused by these two different heating systems.

428 GC/MS data ([Table 3 and Fig. S5 in supplementary material](#)) highlight the similar pattern of the mother liquors
429 obtained by the two different heating systems. In addition to LA, which represents in both cases the main
430 reaction product, as expected, many simple phenols of typical lignin source have been identified. The
431 comparison between the GC/MS data of the two mother liquors confirms the similarity between their chemical
432 composition, not only regarding the FUR and LA concentrations but also considering the lignin fraction, whose
433 degradation released into the water phase phenolic compounds, which are very similar both for type and
434 amount. The identified phenolics were selected as markers for this investigation and quantified as normalized
435 (%) gas chromatographic areas. Because of the ascertained similarity between the two synthesized hydrochars,
436 only that deriving from traditional heating was employed for the trapped phenols recovery by successive
437 hydrochar washing cycles. Four washing fractions were recovered and analyzed by the same gas
438 chromatographic method, in order to quantify their phenolic compounds, taking as reference those of the mother
439 liquor. It was found that the recovery of water-soluble phenolics from the hydrochar was complete after two
440 washing cycles. Anyway, all the recovered fractions were analyzed for total phenolic content (TPC) and
441 antioxidant activity (AA) together with the starting mother liquor, in order to evaluate the response of the adopted
442 methods and data correlations.

443

444 [Table 3, near here](#)

445

446 3.5. Lignin in the liquid phase: total phenolic content (TPC) and antioxidant activity

447 First of all, the overall amount of water-soluble phenolics in the mother liquor was estimated by UV-Vis
448 spectroscopy, as measured after NREL hydrolysis procedure (Licursi et al., 2015), resulting 1.4 wt%, evaluated
449 respect to the starting dried biomass. Then, water soluble fractions recovered from hydrochar washings were
450 analyzed for the yield of soluble compounds (SC), the total phenolic content (expressed as gallic acid equivalent
451 "GAE") and the antioxidant activity, evaluated on the basis of different essays, e.g. TEAC or FRAP. Furthermore,
452 the starting mother liquor was analyzed by the same methods, in order to evaluate the effectiveness of phenols
453 removal by subsequent hydrochar washings. The obtained results are reported in Table 4:

454

455

Table 4, near here

456

457 SC content in the mother liquor was 14.48 g SC/100 g RM, and SC yield increased in 7.1% up to 15.51 g
458 SC/100 g RM with the first washing, and up to 7.5% taking into account a second rinsing. Successive washings
459 diluted and did not improve the soluble solid yield significantly, which resulted in 15.6 g SC/100 g RM.

460 The mother liquor yielded a TPC of 3.16 g of GAE/100g of *Arundo Donax* L. The first rinsing of treated solids
461 recovered an embedded phenolic fraction being the total phenolic yield raised in 7.1%, reaching up to the
462 amount of 3.38 g GAE/100 g RM. The second rinsing increased this yield up to 8.45%. The successive washings
463 improved the total phenolic yield up to 3.48 g GAE/ 100 g RM.

464 Conde et al. (2011) have proposed the recovery of antioxidants from selected lignocellulosic wastes subjected to
465 hydrothermal processing (autohydrolysis). The authors reported solid yields of 28.01-11.52 g SC/100 g of
466 corncobs, 15.6-10.1 g SC/100 g of Eucalypt wood or 31.2-10.9 g SC/100 g of almond shells, in the range of 200-
467 240 °C. The correspondent yields of phenolic compounds were 1.53-2.39 g GAE/100 g of corncobs, 1.31-1.92 g
468 GAE/100 g of Eucalypt wood and 2.06-3.62 g GAE/100 g of almond shells, respectively. Wen et al. (2013)
469 reported that autohydrolysis allowed the solubilization of about 27 g/100 g bamboo culms, and the solubilization
470 of phenolic compounds reached about 3.16 g GAE/100 g RM. This result was higher than those reported by
471 González et al. (2016) starting from autohydrolysis of broom branches (*Cytisus scoparius*). Sipponen et al.
472 (2014) reported that similar phenolic yields in phenolic compounds were obtained from wheat straw during the
473 autohydrolysis pretreatments carried out between 190 and 200 °C. It is worth to note that in the data obtained in

474 our work, lower recoveries in SC yielded higher yields in total phenolic compounds, compared to the results
475 reported in the cited literature.

476 The above data were reprocessed, in order to verify the absence of possible interfering compounds in the
477 analyzed solutions. These data are reported in Fig. 6:

478

479  Fig. 6, near here

480

481 The above figure highlights a well linear correlation between the TEAC and FRAP values and the concentration
482 of phenolic compounds solubilized in the mother liquor and washing recovered. As expected from its phenolic
483 concentration, the mother liquor showed the best values with 1.13 mmol/L of trolox equivalents and 13.5 mmol/L
484 of ascorbic acid equivalents for TEAC and FRAP assays, respectively. Furthermore, the antioxidant capacities of
485 liquors showed a good correlation between the FRAP values and the TEAC values. A strong correlation between
486 antioxidant capacity and total phenolic content (Folin-Ciocalteu) was also obtained, indicating that phenolic
487 compounds mainly contribute to the antioxidant capacities of these liquors. From the operational standpoint, the
488 third and fourth washings did not provide significant increases in the total soluble recovery and their antioxidant
489 activities. The FRAP value obtained for the *Arundo Donax* L. mother liquor was higher than that obtained for the
490 *Acacia ncolitica* (Rajurkar and Hande, 2011). Al-Laith et al. (2015) reported FRAP values in *Aizoon canariense*
491 *L.*, *Asphodelus tenuifolius Cav.*, and *Emex spinosus*, falling within the range of the first *Arundo Donax* L.
492 hydrochar washing. Fig. 7 shows the phenolic concentration effect on the DPPH radical scavenging activity,
493 expressed as inhibition percentage (IP%), which represents the amount of DPPH free radical scavenged from its
494 initial concentration by the same assay.

495

496  Fig. 7, near here

497

498 As expected, the mother liquor and the first washing showed the most active radical scavenger capacities
499 against DPPH radical. It can be observed that the content of phenolics in the extracts is well correlated with their
500 radical scavenger activity. This conclusion suggests that the phenolic compounds which have been
501 independently identified by GC/MS analysis (Table 2) significantly contribute to the overall antioxidant capacity,
502 in agreement with the reported positive correlation between phenolic concentration and antioxidant activity

503 (Espinoza-Acosta et al., 2016; Turumtay et al., 2014). In particular, lignin degradation, which has occurred
504 during the acid-catalysed hydrothermal treatment, has released simple phenolic compounds, which have been
505 independently identified by GC/MS, such as phenolic alcohols (guaiacol, syringol), as well as phenolic acids
506 (syringic acid, vanillic acid, hydrobenzoic acid) and aldehydes (syringaldehyde), which predominantly contribute
507 to the overall antioxidant activity. These bioactive compounds can be subsequently isolated by different
508 traditional strategies, mainly including solvent extraction, adsorption-desorption, **supercritical extraction** and
509 membrane processing (Conde et al., 2017; Egües et al., 2012, Moure et al., 2014; Parajó et al., 2008, Um et al.,
510 2017), and research on this topic is in progress.

511

512 **4. Conclusions**

513 **This research has clarified the chemical composition of the simple phenolics of lignin source present in the solid**
514 **and liquid fractions, obtained after the acid-catalysed hydrothermal treatment of giant reed (*Arundo Donax* L.).**
515 **Traditional (autoclave) and microwave heating systems were compared, revealing a similarity between the**
516 **chemical profile of the phenolic compounds in both fractions. The investigation of the solid phase (hydrochar)**
517 **was carried out by different analytical techniques, Py-GC/MS, TGA/FTIR, and EGA-MS, confirming the**
518 **possibility of an additional recovery of simple phenolic compounds, deriving from the further thermal degradation**
519 **of the hydrochar. On the other hand, the liquid fractions, e.g. the mother liquor and the hydrochar washings,**
520 **were analyzed by GC/MS, identifying many simple phenolic compounds, directly deriving from the acid-catalysed**
521 **hydrothermal treatment of the starting biomass. Moreover, mother liquor and the water washings were analyzed**
522 **for the total phenolic content (TPC) and antioxidant activity (AA), adopting TEAC, FRAP, and DPPH standard**
523 **assays. Promising antioxidant properties were ascertained for the mother liquor and the first two hydrochar**
524 **washing cycles, obtaining good linear correlations between total phenolic compounds (TPC) and antioxidant**
525 **capacity (TEAC, FRAP, and DPPH). This new approach can significantly contribute to improving the**
526 **sustainability of the entire LA process, up to now targeted for the LA production, focusing the attention towards**
527 **new niche bioproducts, the antioxidants, which surely add significant economic value to the overall Biorefinery of**
528 **the lignocellulosic biomass.**

529

530 **Acknowledgments**

531 The authors gratefully acknowledge the financial support by the Bank Foundation “Cassa di Risparmio” of Lucca,
532 under “VALCELL” Project. Dr. Rudy Parton of GF Biochemicals is gratefully acknowledged for helpful
533 discussions.

534

535 **References**

536 Al-Laith, A.A., Alkhuzai, J., Freije, A., 2015. Assessment of antioxidant activities of three wild medicinal plants
537 from Bahrain. *Arabian J. Chem.* DOI:10.1016/j.arabjc.2015.03.004.

538 Antonetti, C., Bonari, E., Licursi, D., Nassi, N., Raspolli Galletti, A.M., 2015. Hydrothermal conversion of giant
539 reed to furfural and levulinic acid: Optimization of the process under microwave irradiation and investigation
540 of distinctive agronomic parameters. *Molecules* 20, 21232–21253.

541 Antonetti, C., Licursi, D., Fulignati, S., Valentini, G., Raspolli Galletti, A.M., 2016. New frontiers in the catalytic
542 synthesis of levulinic acid: from sugars to raw and waste biomass as starting feedstock. *Catalysts* 6, 196-225.

543 Antonetti, C., Melloni, M., Licursi, D., Fulignati, S., Ribechini, E., Rivas, S., Parajó, J.C., Cavani, F., Raspolli
544 Galletti, A.M., 2017a. Microwave-assisted dehydration of fructose and inulin to HMF catalyzed by niobium
545 and zirconium phosphate catalysts. *Appl. Catal., B* 206, 364-377.

546 Antonetti, C., Raspolli Galletti, A.M., Fulignati, S., Licursi, D., 2017b. Amberlyst A-70: A surprisingly active
547 catalyst for the MW-assisted dehydration of fructose and inulin to HMF in water. *Catal. Commun.* 97, 146-
548 150.

549 Benzie, I.F.F., Strain, J.J. 1996. The ferric reducing ability of plasma (FRAP) as a measure of “antioxidant
550 power”: The FRAP assay. *Anal. Biochem.* 239, 70–76.

551 Bernardini, J., Licursi, D., Anguillesi, I., Cinelli, P., Coltelli, M.B., Antonetti, C., Raspolli Galletti, A.M., Lazzeri, A.,
552 2017. Exploitation of *Arundo Donax* L. hydrolysis residue for the green synthesis of flexible polyurethane
553 foams. *BioRes.* 12, 3630-3655.

554 Bernal, H.G., Bernazzani, L., Raspolli Galletti, A.M., 2014. Furfural from corn stover hemicelluloses. A mineral
555 acid-free approach. *Green Chem.* 16, 3734-3740.

556 Bosco, S., Nassi, N., Roncucci, N., Mazzoncini, M., Bonari, E., 2016. Environmental performances of giant reed
557 (*Arundo Donax L.*) cultivated in fertile and marginal lands: A case study in the Mediterranean. *Eur. J. Agron.*
558 78, 20–31.

559 Conde, E., Moure, A., Domínguez, H., Parajó, J.C., 2008. Fractionation of antioxidants from autohydrolysis of
560 barley husks. *J. Agric. Food Chem.* 56, 10651–10659.

561 Conde, E., Moure, A., Domínguez, H., Parajó, J.C., 2011. Production of antioxidants by non-isothermal
562 autohydrolysis of lignocellulosic wastes. *LWT - Food Sci. Technol.* 44, 436-442.

563 Conde, E., Moure, A., Domínguez, H., 2017. Recovery of phenols from autohydrolysis liquors of barley husks:
564 kinetic and equilibrium studies. *Ind. Crops Prod.* 103, 175-184.

565 Egües, I., Sanchez, C., Mondragon, I., Labidi, J., 2012. Antioxidant activity of phenolic compounds obtained by
566 autohydrolysis of corn residues. *Ind. Crops Prod.* 36, 164-171.

567 Espinoza-Acosta, J.L., Torres-Chávez, P.I., Ramírez-Wong, B., López-Saiz, C.M., Montañó-Leyva, B., 2016.
568 Antioxidant, antimicrobial, and antimutagenic properties of technical lignins and their applications. *BioRes.*
569 11, 5452-5481.

570 Filiciotto, L., Balu, A.M., Van der Waal, J.C., Luque, R., 2017. Catalytic insights into the production of biomass-
571 derived side products methyl levulinate, furfural and humins. *Catal. Today*. DOI:
572 10.1016/j.cattod.2017.03.008.

573 Freitas, F.A., Licursi, D., Lachter, E.R., Raspolli Galletti, A.M., Antonetti, C., Brito, T.C., Nascimento, R.S.V.,
574 2016. Heterogeneous catalysis for the ketalization of ethyl levulinate with 1,2- dodecanediol: Opening the
575 way to a new class of bio-degradable surfactants. *Catal. Commun.* 73, 84-87.

576 Galia, A., Schiavo, B., Antonetti, C., Raspolli Galletti, A.M., Interrante, L., Lessi, M., Scialdone, O., Valenti, M.G.,
577 2015. Autohydrolysis pretreatment of *Arundo donax*: a comparison between microwave-assisted batch and
578 fast heating rate flow-through reaction systems. *Biotechnol. Biofuels.* 8, 218-235.

579 Garrote, G., Falqué, E., Domínguez, H., Parajó, J.C., 2007. Autohydrolysis of agricultural residues: Study of
580 reaction byproducts. *Biores. Technol.* 98, 1951-1957.

581 GFBiochemicals, 2017. <http://www.gfbiochemicals.com> (accessed 1 May, 2017).

582 González, N., Otero, A., Conde, E., Falqué, E., Moure, A., Domínguez, H., 2016. Extraction of phenolics from
583 broom branches using green technologies. *J. Chem. Technol. Biotechnol.* 92, 1345-1352.

584 Grilc, M., Likozar, B., Levec, J., 2014a. Hydrotreatment of solvolytically liquefied lignocellulosic biomass over
585 NiMo/Al₂O₃ catalyst: Reaction mechanism, hydrodeoxygenation kinetics and mass transfer model based on
586 FTIR. *Biomass Bioenergy* 63, 300-312.

587 Grilc, M., Likozar, B., Levec, J., 2014b. Hydrodeoxygenation and hydrocracking of solvolysed lignocellulosic
588 biomass by oxide, reduced and sulphide form of NiMo, Ni, Mo and Pd catalysts. *Appl. Catal. B. Environ.* 150-
589 151, 275-287.

590 Grilc, M., Likozar, B., Levec, J., 2015. Kinetic model of homogeneous lignocellulosic biomass solvolysis
591 inglycerol and imidazolium-based ionic liquids with subsequent heterogeneous hydrodeoxygenation over
592 NiMo/Al₂O₃ catalyst. *Catal. Today* 256, 302-314.

593 Hayes, D.J., Fitzpatrick, S., Hayes, M.H.B., Ross, J.R.H., 2006. The Biofine process – Production of levulinic
594 acid, furfural, and formic acid from lignocellulosic feedstocks, in: Kamm, B., Gruber, P.R., Kamm, M. (Eds.),
595 Biorefineries – Industrial processes and products: status quo and future directions. WILEY-VCH Verlag
596 GmbH, Weinheim, pp. 139-164.

597 Heltzel, J., Patil, S.K.R., Lund, C.R.F., 2016. Humin formation pathways, in: Schlaf, M., Zhang, Z.C. (Eds.),
598 Reaction pathways and mechanisms in thermocatalytic biomass conversion II. Springer, Singapore, pp. 105-
599 118.

600 Jin, F., Enomoto, H., 2011. Rapid and highly selective conversion of biomass into value-added products in
601 hydrothermal conditions: chemistry of acid/base catalyzed and oxidation reactions. *Energy Environ. Sci.* 4,
602 382–397.

603 Jin, F., Wang, Y., Zeng, X., Shen, Z., Yao, G., 2014. Water under high temperature and pressure conditions and
604 its applications to develop green technologies for biomass conversion, in: Jin, F. (Ed.), Application of
605 hydrothermal reactions to biomass conversion. Springer-Verlag, Berlin, pp. 3-28.

606 Kang, S., Li, X., Fan, J., Chang, J., 2013. Hydrothermal conversion of lignin: A review. *Renew. Sust. Energ. Rev.*
607 27, 546–558.

608 Licursi, D., Antonetti, C., Bernardini, J., Cinelli, P., Coltelli, M.B., Lazzeri, A., Martinelli, M., Raspolli Galletti, A.M.,
609 2015. Characterization of the *Arundo Donax* L. solid residue from hydrothermal conversion: comparison with
610 technical lignins and application perspectives. *Ind. Crops Prod.* 76, 1008-1024.

611 Licursi, D., Antonetti, C., Fulignati, S., Vitolo, S., Puccini, M., Ribechini, E., Bernazzani, L., Raspolli Galletti, A.M.,
612 2017. Multivalorisation of waste hazelnut shells: hydrothermal conversion to levulinic acid and production of
613 valuable hydrochar. *Bioresour. Technol.* **244**, 880-888.

614 Mattonai, M., Tamburini, D., Colombini, M.P., Ribechini, E., 2016. Timing in analytical pyrolysis: Py(HMDS)-
615 GC/MS of glucose and cellulose using online micro reaction sampler. *Anal. Chem.* **88**, 9318-9325.

616 Moure, A., Conde, E., Falqué, E., Domínguez, H., Parajó, J.C., 2014. Production of nutraceuticals from chestnut
617 burs by hydrolytic treatment. *Food Res. Int.* **65**, 359-366.

618 Mukherjee, A., Dumont, M.-J., Raghavan, V., 2015. Review: Sustainable production of hydroxymethylfurfural and
619 levulinic acid: challenges and opportunities. *Biomass Bioenerg.* **72**, 143-183.

620 Parajó, J.C., Domínguez, H., Moure, A., Díaz-Reinoso, B., Conde, E., Soto, M.L., Conde, M.J., González-López,
621 N., 2008. Recovery of phenolic antioxidants released during hydrolytic treatments of agricultural and forest
622 residues. *Electron. J. Environ. Agric. Food Chem.* **7**, 3243-3249.

623 Parton, R.F.M.J., Rijkers, M.P.W.M., Kroon, J.A., 2013. Continuous production of furfural and levulinic acid.
624 US8426619 B2.

625 Pavlovič, I., Knez, Ž., Škerget, M., 2013. Hydrothermal reactions of agricultural and food processing wastes in
626 sub- and supercritical water: a review of fundamentals, mechanisms, and state of research. *J. Agric. Food*
627 *Chem.* **61**, 8003–8025.

628 Pileidis, F.D., Titirici, M.M., 2016. Levulinic acid biorefineries: new challenges for efficient utilization of biomass.
629 *ChemSusChem* **9**, 562-582.

630 Rajurkar, N.S., Hande, S.M., 2011. Estimation of phytochemical content and antioxidant activity of some
631 selected traditional Indian medicinal plants. *Indian J. Pharm. Sci.* **73**, 146–151.

632 Re, R., Pellegrini, N., Proteggente, A., Pannala, A., Yang, M., Rice-Evans, C., 1999. Antioxidant activity applying
633 an improved ABTS radical cation decolorization assay. *Free Radic. Biol. Med.* **26**, 1231–1237.

634 Ribechini, E., Zanaboni, M., Raspolli Galletti, A.M., Antonetti, C., Nassi, N., Bonari, E., Colombini, M.P., 2012.
635 Py-GC/MS characterization of a wild and a selected clone of *Arundo Donax*, and of its residues after catalytic
636 hydrothermal conversion to high added-value products. *J. Anal. Appl. Pyrol.* **94**, 223–229.

637 Ribechini, E., Mangani, F., Colombini, M.P., 2015. Chemical investigation of barks from broad-leaved tree
638 species using EGA-MS and GC/MS. *J. Anal. Appl. Pyrol.* **114**, 235-242.

639 Rivas, S., Raspolli-Galletti, A.M., Antonetti, C., Santos, V., Parajó, J.C., 2015. Sustainable production of levulinic
640 acid from the cellulosic fraction of *Pinus Pinaster* wood: Operation in aqueous media under microwave
641 irradiation. *J. Wood Chem. Technol.* 35, 315-324.

642 Rivas, S., Raspolli-Galletti, A.M., Antonetti, C., Santos, V., Parajó, J.C., 2016. Sustainable conversion of *Pinus*
643 *pinaster* wood into biofuel precursors: A biorefinery approach. *Fuel* 164, 51-58.

644 Savy, D., Nebbioso, A., Mazzei, P., Drosos, M., Piccolo, A., 2015a, Molecular composition of water-soluble
645 lignins separated from different non-food biomasses. *Fuel Process. Technol.* 131, 175–181.

646 Savy, D., Cozzolino, V., Vinci, G., Nebbioso, A., Piccolo, A., 2015b. Water-soluble lignins from different
647 bioenergy crops stimulate the early development of maize (*Zea mays* L.). *Molecules* 20, 19958–19970.

648 Savy, D., Cozzolino, V., Nebbioso, A., Drosos, M., Nuzzo, A., Mazzei, P., Piccolo, A., 2016. Humic-like
649 bioactivity on emergence and early growth of maize (*Zea mays* L.) of water-soluble lignins isolated from
650 biomass for energy. *Plant Soil* 402, 221–233.

651 **Silva, J.F.L., Grekin, R., Mariano, A.P., Filho, R.M., 2017. Making levulinic acid and ethyl levulinate economically**
652 **viable: a worldwide techno-economic and environmental assessment of possible routes. *Energy Technol.***
653 **DOI: 10.1002/ente.201700594.**

654 Singleton, V.L., Rossi, J.A., 1965. Colorimetry of total phenolics with phosphomolybdic-phosphotungstic acid
655 reagents. *Am. J. Enol. Vitic.* 16, 144–158.

656 Sipponen, M.H., Pihlajaniemi, V., Sipponen, S., Pastinen, O., Laakso, S., 2014. Autohydrolysis and aqueous
657 ammonia extraction of wheat straw: effect of treatment severity on yield and structure of hemicellulose and
658 lignin. *RSC Adv.* 4, 23177-23184.

659 **Sluiter, A., Hames, B., Hyman, D., Payne, C., Ruiz, R., Scarlata, C., Sluiter, J., Templeton, D., Wolfe, J., 2008.**
660 **Determination of total solids in biomass and total dissolved solids in liquid process samples. Laboratory**
661 **analytical procedure (LAP). Technical Report NREL/TP-510-42621.**

662 **Sumerskii, I.V., Krutov, S.M., Zarubin, M.Ya., 2010. Humin-like substances formed under the conditions of**
663 **industrial hydrolysis of wood. *Russ. J. Appl. Chem.* 83, 320–327.**

664 Tamburini, D., Łucejko, J.J., Ribechini, E., Colombini, M.P., 2015. Snapshots of lignin oxidation and
665 depolymerization in archaeological wood: an EGA-MS study. *J. Mass Spectrom.* 50, 1103-1113.

666 Tsilomelekis, G., Orella, M.J., Lin, Z., Cheng, Z., Zheng, W., Nikolakis, V., Vlachos, D.G., 2016. Molecular
667 structure, morphology and growth mechanisms and rates of 5-hydroxymethyl furfural (HMF) derived humins.
668 Green Chem. 18, 1983-1993.

669 Turumtay, E.A., İslamoğlu, F., Çavuş, D., Şahin, H., Turumtay, H., Vanholme, B., 2014. Correlation between
670 phenolic compounds and antioxidant activity of Anzer tea (*Thymus praecox* Opiz subsp. *caucasicus* var.
671 *caucasicus*). Ind. Crops Prod. 52, 687-694.

672 Um, M., Shin, G.-J., Lee, J.-W., 2017. Extraction of total phenolic compounds from yellow poplar hydrolysate and
673 evaluation of their antioxidant activities. Ind. Crops Prod. 97, 574-581.

674 Van der Waal, J.C., De Jong, E., 2016. Avantium chemicals: The high potential for the levulinic product tree, in:
675 de María, P.D. (Ed.), Industrial biorenewables: a practical viewpoint. John Wiley & Sons, Hoboken, pp. 97-
676 120.

677 Van Zandvoort, I., Wang, Y., Rasrendra, C.B., van Eck, E.R.H., Bruijninx, P.C.A., Heeres, H.J., Weckhuysen,
678 B.M., 2013. Formation, molecular structure, and morphology of humins in biomass conversion: influence of
679 feedstock and processing conditions, ChemSusChem 6, 1745–1758.

680 Wang, L., Cheng, D., 2014. Biomass pyrolysis and bio-oil utilization, in: Wang, L. (Ed.), Sustainable Energy
681 Production. CRC Press, Taylor & Francis Group, Boca Raton, Chapter 18, pp. 361-378.

682 Wang, S., Lin, H., Zhao, Y., Chen, J., Zhou, J., 2016. Structural characterization and pyrolysis behavior of humin
683 by-products from the acid-catalysed conversion of C6 and C5 carbohydrates. J. Anal. Appl. Pyrol. 118, 259-
684 266.

685 Wang, S., Luo, Z., 2017. Pyrolysis of lignin, in: Wang, S., Luo, Z. (Eds.), Pyrolysis of biomass. Walter de Gruyter
686 GmbH, Berlin, pp. 103-140.

687 Wang, H., Tucker, M., Ji, Y., 2013. Recent development in chemical depolymerization of lignin: A review. J. Appl.
688 Chem. DOI: 10.1155/2013/838645.

689 Watkins, D., Nuruddin, M., Hosur, M., Tcherbi-Narteh, A., Jeelani, S., 2015. Extraction and characterization of
690 lignin from different biomass resources. J. Mater. Res. Technol. 4, 26-32.

691 Wen, J.-L., Sun, S.-N., Yuan, T.-Q., Xu, F., Sun, R.-C., 2013. Fractionation of bamboo culms by autohydrolysis,
692 organosolv delignification and extended delignification: Understanding the fundamental chemistry of the lignin
693 during the integrated process. Bioresour. Technol. 150, 278–286.

694 Yao, Z., Ma, X., Wu, Z., Yao, T., 2017. TGA–FTIR analysis of co-pyrolysis characteristics of hydrochar and
695 paper sludge. *J. Anal. Appl. Pyrol.* 123, 40-48.

696 You, T.-T., Mao, J.-Z., Yuan, T.-Q., Wen, J.-L., Xu, F., 2013. Structural elucidation of the lignins from stems and
697 foliage of *Arundo Donax* Linn.. *J. Agric. Food Chem.* 61, 5361–5370.

698 Zhang, L., Yan, L., Wang, Z., Laskar, D.D., Swita, M.S., Cort, J.R., Yang, B., 2015. Characterization of lignin
699 derived from water-only and dilute acid flowthrough pretreatment of poplar wood at elevated temperatures.
700 *Biotechnol. Biofuels* DOI: 10.1186/s13068-015-0377-x.

701 Zhuang, J., Wang, X., Xu, J., Wang, Z., Qin, M., 2017. Formation and deposition of pseudo-lignin on liquid hot-
702 water-treated wood during the cooling process. *Wood Sci. Technol.* 51, 165–174.

703

704

705

706

707

708

709

710

711

712

713

714

715

716

717

718 **Table 1** LA and hydrochar mass data yield obtained from the optimized Arundo Donax L. hydrolysis reactions,
719 carried out in microwave and autoclave reactors at 190 °C.

| Heating system | Time (min.) | LA mass yield (wt%) | % on theoretical LA yield | Hydrochar mass yield (wt%) |
|-----------------------|--------------------|----------------------------|----------------------------------|-----------------------------------|
| Microwave | 20 | 21.3 | 75.4 | 28.9 |
| Autoclave | 60 | 22.1 | 78.2 | 29.7 |

720

721

722

723

724

725

726

727

728

729

730

731

732

733

734

735

736

737

738

739

740

741

742 **Table 2** Identification of the pyrolysis products for the microwave- and autoclave- derived *Arundo Donax* L.
 743 hydrochars, under the best reaction conditions for LA synthesis. N° refers to the peak numeration reported in
 744 Fig. 1.

| N° | Name | Microwave (%) | Autoclave (%) | Source |
|----|--|---------------|---------------|--------|
| 1 | Phenol (TMS) | 2.9 | 2.8 | |
| 2 | 2-Hydroxypropanoic acid (2TMS) | 2.0 | 10.0 | |
| 3 | 2-Hydroxyacetic acid (2TMS) | 0.5 | 1.1 | |
| 4 | Guaiacol | 0.3 | 0.0 | G |
| 5 | <i>o</i> -Cresol (TMS) | 0.5 | 0.7 | |
| 6 | Levulinic acid (TMS) | 16.7 | 15.4 | |
| 7 | <i>m</i> -Cresol (TMS) | 4.2 | 0.3 | |
| 8 | Methyl-guaiacol | 0.2 | 0.0 | G |
| 9 | 1,2-Dihydroxybenzene (TMS) | 0.6 | 0.2 | |
| 10 | Guaiacol (TMS) | 6.5 | 4.9 | G |
| 11 | Hydroxyxylene (TMS) | 3.4 | 2.3 | |
| 12 | Phosphate (3TMS)* | --- | --- | |
| 13 | Butanedioic acid (2 TMS) | 4.1 | 12.8 | |
| 14 | 1,2-Dihydroxybenzene (2TMS) | 1.2 | 0.0 | |
| 15 | 4-Methylguaiacol (TMS) | 13.0 | 0.5 | G |
| 16 | 2-Methyl-3-hydroxy-(4H)-pyran-4-one (TMS) | 0.1 | 0.0 | |
| 17 | 1,4-Dihydroxybenzene (2TMS) | 0.1 | 0.0 | |
| 18 | 4-Methylcatechol (2TMS) | 1.5 | 1.8 | G |
| 19 | 4-Ethylguaiacol (TMS) | 2.9 | 1.5 | G |
| 20 | Syringol (TMS) | 4.0 | 3.7 | G |
| 21 | 4-Vinylguaiacol (TMS) | 5.3 | 6.4 | G |
| 22 | 4-Ethylcatechol (2TMS) | 0.3 | 0.3 | G |
| 23 | Eugenol (TMS) | 0.3 | 0.6 | G |
| 24 | 4-Methylsyringol (TMS) | 7.7 | 6.1 | G |
| 25 | E-Isoeugenol (TMS) | 0.1 | 0.2 | G |
| 26 | Vanillin (TMS) | 1.1 | 2.8 | G |
| 27 | 1,2,3-Trihydroxybenzene (3TMS) | 0.3 | 0.0 | |
| 28 | 5-Methyl-3-methoxy-1,2-benzenediol (2TMS) | 1.9 | 1.7 | |
| 29 | 4-Ethylsyringol (TMS) | 0.7 | 0.4 | S |
| 30 | Z-Isoeugenol (TMS) | 1.3 | 1.9 | G |
| 31 | 4-Vinylsyringol (TMS) | 1.9 | 2.5 | S |
| 32 | 1,2,4-Trihydroxybenzene (3TMS) | 0.8 | 0.5 | |
| 33 | Acetovanillone (TMS) | 1.1 | 0.8 | G |
| 34 | 4-Hydroxy benzoic acid (2TMS) | 0.2 | 0.4 | |
| 35 | 4-Hydroxy-3,5-dimethoxy cinnamic acid methyl ester (TMS) | 0.3 | 0.3 | S |
| 36 | Syringaldehyde (TMS) | 1.1 | 2.2 | S |
| 37 | E-Propenylsyringol (TMS) | 0.8 | 1.2 | S |

| | | | | |
|----|---|-----|-----|---|
| 38 | Vanillic acid (2TMS) | 3.7 | 4.7 | G |
| 39 | Acetosyringone (TMS) | 1.1 | 1.3 | S |
| 40 | Z-Coniferyl alcohol (2TMS) | 0.2 | 0.3 | G |
| 41 | Syringic acid (2TMS) | 1.8 | 2.7 | S |
| 42 | E-Coniferyl alcohol (2 TMS) | 2.0 | 2.4 | G |
| 43 | Syringylpropanol (2TMS) | 0.1 | 0.5 | S |
| 44 | 3,4-Dihydroxy cinnamyl alcohol (3TMS) | 0.0 | 0.1 | G |
| 45 | Palmitic acid (TMS) * | --- | --- | |
| 46 | E-Synapyl alcohol (2TMS) | 1.2 | 1.7 | S |
| 47 | E-2-Methoxy-3,4-dihydroxy cinnamic alcohol (3TMS) | 0.1 | 0.1 | G |
| 48 | Stearic acid (TMS) * | --- | --- | |

745

746

Note a: "G" refers to the pyrolysis products deriving from coniferyl lignin units, and "S" to those from syringyl ones.

747

748

749

750

751

752

753

754

755

756

757

758

759

760

761

762

763

764

765 **Table 3** Compounds identified (by GC/MS) in the mother liquors recovered after *Arundo Donax* L. hydrolysis in
 766 microwave and autoclave systems, under the best reaction conditions. N° refers to the numbers of the peaks
 767 which are correspondingly reported in Figure 7.

| N° | Compound | m/z |
|----|--|---|
| 1 | Levulinic acid 2TMS | 188, 173, 155, 145, 131, 129, 99, 75 |
| 2 | Unknown I | 202, 187, 160, 143, 129, 112, 75 |
| 3 | 1,2-dihydroxybenzene TMS | 182, 167, 166, 151, 136, 91, 75 |
| 4 | Unknown II | 202, 187, 173, 159, 145, 131, 75, 73 |
| 5 | Guaiacol TMS | 196, 181, 166, 151, 136 |
| 6 | 3-hydroxy-6-methyl-(2H)-pyran-2-one TMS | 198, 183, 111, 73 |
| 7 | (E/Z)-2,4-dihydroxypent-2-enal 2TMS | 260, 245, 217, 147, 143, 73 |
| 8 | (E/Z)-2,4-dihydroxypent-2-enal 2TMS | 260, 245, 217, 147, 143, 73 |
| 9 | 2,4-dihydroxypentanal 2TMS | 262, 247, 147, 129, 73 |
| 10 | 1,2-dihydroxybenzene 2TMS | 254, 239, 166, 151, 136, 73 |
| 11 | Propanedioic acid 2TMS | 276, 261, 232, 217, 204, 186, 147, 73 |
| 12 | Unknown III | 276, 261, 233, 190, 171, 159, 147, 133, 103, 73 |
| 13 | 3-hydroxy-2-hexenoic acid 2TMS | 274, 259, 230, 215, 147, 75, 73 |
| 14 | 1,4-dihydroxybenzene 2TMS | 254, 239 |
| 15 | Syringol TMS | 226, 211, 196, 151, 153, 73 |
| 16 | 3-hydroxyacetophenone TMS | 208, 193, 165, 151, 135, 123, 105, 91, 73 |
| 17 | 2,3-dihydroxycyclopent-2-enone 2TMS | 258, 243, 73 |
| 18 | 4-hydroxyacetophenone TMS | 208, 193, 151, 135, 89, 73 |
| 19 | 3-methoxy-1,2-benzenediol 2TMS | 284, 269, 254, 239, 153, 73 |
| 20 | Unknown IV | 222, 207, 179, 163, 149 |
| 21 | Butylated hydroxytoluene | 220, 205, 177, 145, 105, 91, 57 |
| 22 | Vanillin TMS | 224, 209, 194, 179, 163 |
| 23 | Unknown V | 240, 225, 196, 181, 165, 150, 73 |
| 24 | 3-hydroxybenzoic acid 2TMS | 282, 267, 223, 193, 149, 91, 73 |
| 25 | Unknown VI | 243, 240, 225, 216, 215, 198, 197, 183, 173, 129, 126, 123, 113, 111, 109, 95, 85, 75, 73, 55 |
| 26 | Acetovanillone TMS | 238, 223, 208, 193, 73 |
| 27 | 4-hydroxybenzoic acid 2TMS | 282, 267, 223, 207, 193, 73 |
| 28 | 3-(3-methoxy-4-hydroxyphenyl)propanal TMS | 252, 237, 222, 209, 193, 179, 163, 149, 73 |
| 29 | Syringaldehyde TMS | 254, 239, 224, 153 |
| 30 | Tridecanoic acid TMS (IS) | 289, 271, 145, 129, 117, 75, 73 |
| 31 | Vanillic acid 2TMS | 312, 297, 282, 267, 253, 223, 207, 193, 179, 165, 126, 73 |
| 32 | Acetosyringone TMS | 268, 253, 238, 223, 208, 193, 165, 137, 119, 104 |
| 33 | 3-(3,5-dimethoxy-4-hydroxyphenyl)propanal TMS | 282, 267, 252, 239, 209, 179, 166, 151 |
| 34 | Unknown VII | 370, 355, 311, 267, 223, 193, 165, 137 |
| 35 | Unknown VIII | 384, 369, 267, 173, 147, 125, 73 |
| 36 | 3-(3-methoxy-4,5-dihydroxyphenyl)propanal 2TMS | 340, 325, 297, 267, 209, 73 |
| 37 | Syringic acid 2TMS | 342, 327, 312, 297, 283, 253, 223, 141, 73 |
| 38 | Unknown IX | 366, 321, 291, 251, 218, 203, 176, 161, 147, 73 |

| | | |
|----|--|--|
| 39 | 3,4-dihydroxy-5-methoxybenzoic acid 3TMS | 400, 385, 341, 311, 297, 253, 237, 223, 195, 73 |
| 40 | Unknown X | 338, 323, 249, 233, 193, 73 |
| 41 | Unknown XI | 364, 349, 292, 278, 263, 207 |
| 42 | Unknown XII | 276, 261, 219, 203, 73 |
| 43 | Unknown XIII | 366, 351, 193, 173, 73 |
| 44 | Unknown XIV | 426, 411, 396, 381, 223, 193, 173, 73 |
| 45 | Unknown XV | 384, 369, 294, 251, 222, 193, 177, 149, 135, 121, 73 |

768

769

770

771

772

773

774

775

776

777

778

779

780

781

782

783

784

785

786

787

788

789

790

791

792 **Table 4** Soluble compounds, total phenolic content, and antioxidant activity (on basis of TEAC and FRAP
 793 assays) per g of raw biomass, for the mother liquor and hydrochar washings.

| | Soluble Compounds | Total Phenolic Content | TEAC | FRAP |
|---|--------------------------|-------------------------------|-----------------------|----------------------|
| | mg SC/ g RM | mg GAE/g RM | mg trolox/g RM | mg AAE / g RM |
| Mother liquor | 145±1 | 31.6±0.6 | 0.212±0.009 | 35.9±0.7 |
| 1 st Washing | 10.3±0.2 | 2.23±0.06 | 0.053±0.003 | 2.52±0.05 |
| 2 nd Washing | 0.723±0.078 | 0.442±0.005 | 0.068±0.003 | 0.547±0.014 |
| 3 rd Washing | 0.231±0.025 | 0.278±0.005 | 0.023±0.002 | 0.352±0.015 |
| 4 th Washing | 0.225±0.036 | 0.290±0.005 | 0.024±0.000 | 0.375±0.013 |
| Liquor+1 st Washing | 155 | 33.8 | 0.265 | 38.4 |
| Liquor+1 st and 2 nd Washings | 156 | 34.2 | 0.332 | 38.9 |
| Total sum | 156 | 34.8 | 0.379 | 39.7 |

794 RM: Raw Material (biomass). SC: Soluble Compounds. GAE: Gallic Acid Equivalent. AAE: Ascorbic Acid
 795 Equivalent.

796

797

798

799

800

801

802

803

804

805

806

807

808

809

810

811

812 **Figure captions**

813 **Fig. 1** TG and DTG curves of the starting *Arundo Donax* L. and microwave- and autoclave- derived hydrochars,
814 the latter produced under the optimized reaction conditions to give LA.

815 **Fig. 2** 3D FTIR spectra of the gas evolved from the autoclave-derived *Arundo Donax* L. hydrochar.

816 **Fig. 3** Thermograms of the gas evolved from the starting *Arundo Donax* L. and its microwave- and autoclave-
817 derived hydrochars, the latter synthesized under the optimized reaction conditions to give LA.

818 **Fig. 4** Mass spectra of the starting *Arundo Donax* L. biomass obtained by EGA-MS: a) integration time: 10-27
819 min. and b) 27-43 min.

820 **Fig. 5** Mass spectra of the a) microwave- and b) autoclave- derived *Arundo Donax* L. hydrochar obtained by
821 EGA-MS (integration time: 10-43 min).

822 **Fig. 6** Correlation between the concentration of phenolic compounds (expressed as mg GAE/L) and the
823 antioxidant activity assayed by TEAC and FRAP.

824 **Fig. 7** Correlation between the total phenolic compounds and the DPPH radical scavenging activity in the mother
825 liquor and hydrochar washings.

826

Figure 1

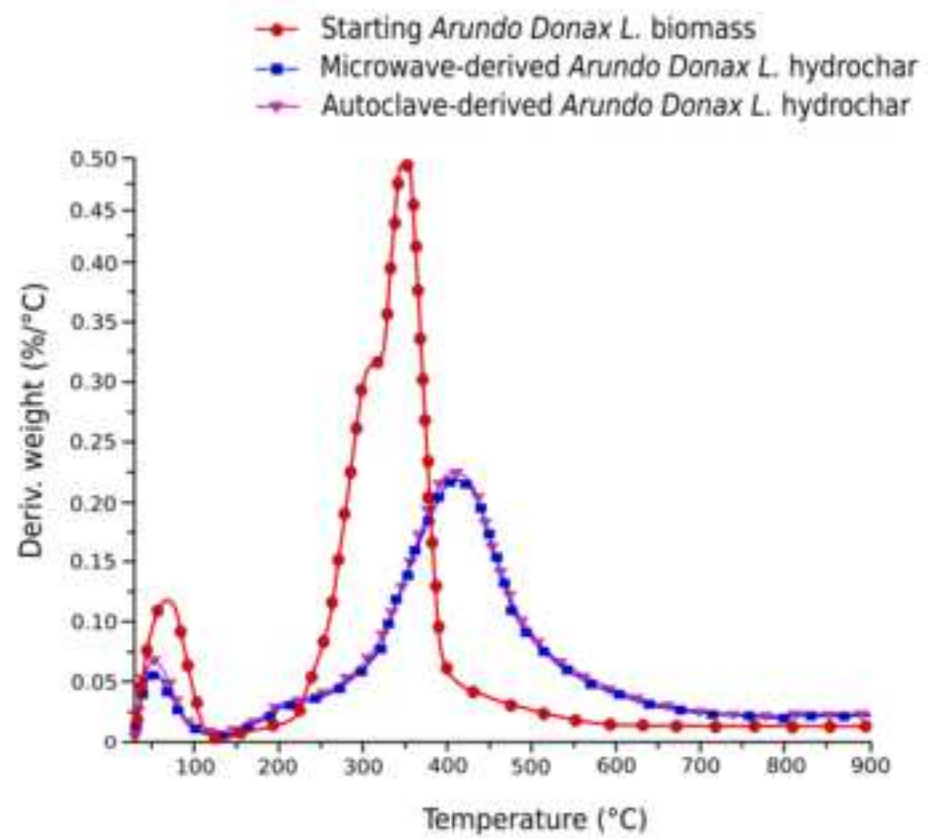
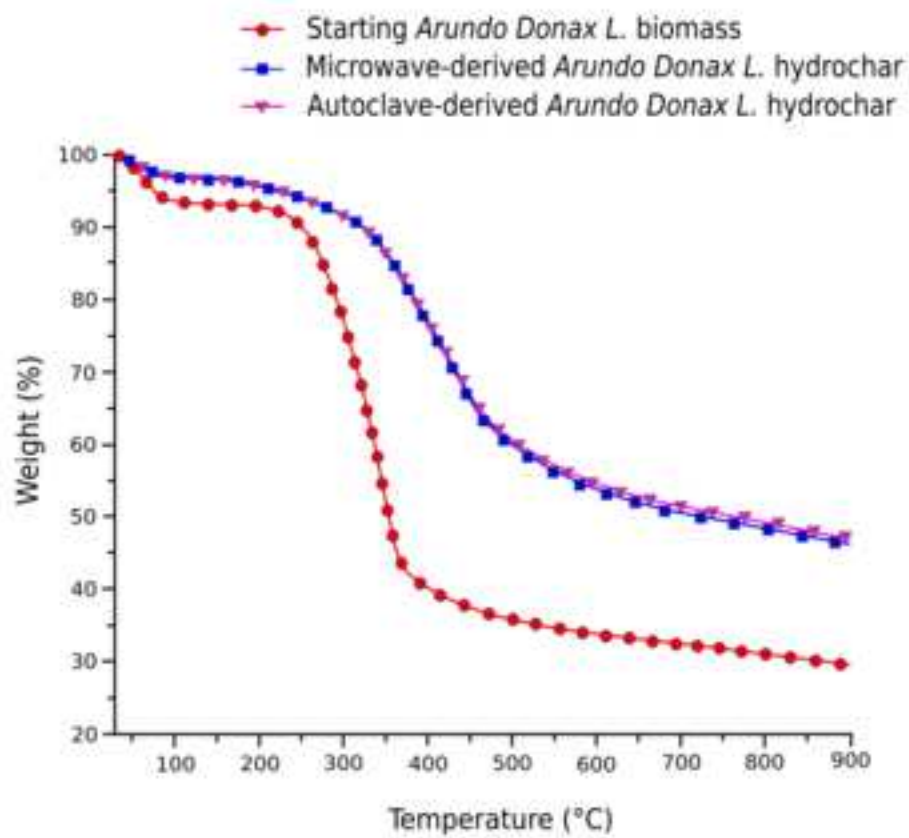


Figure 2

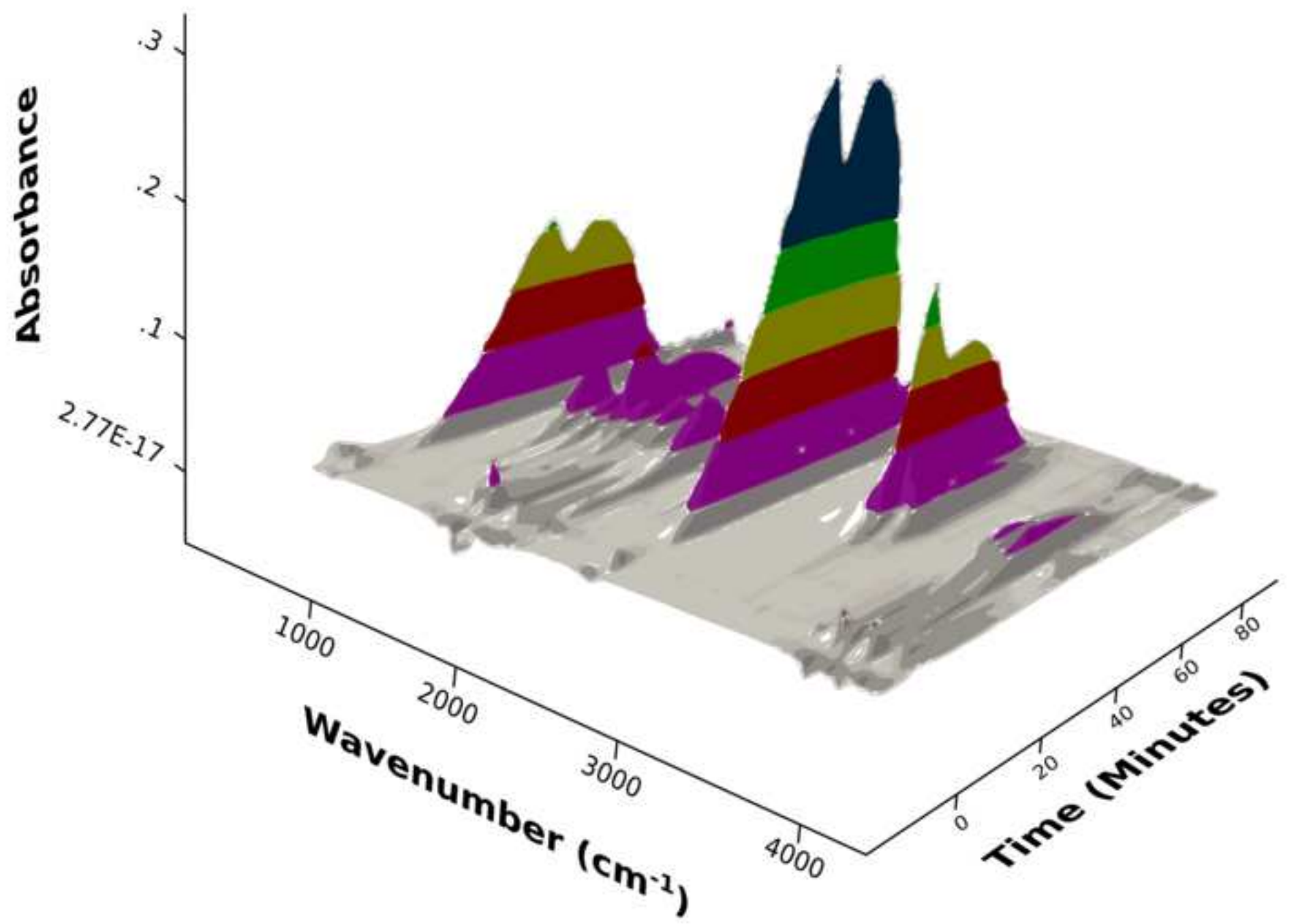


Figure 3

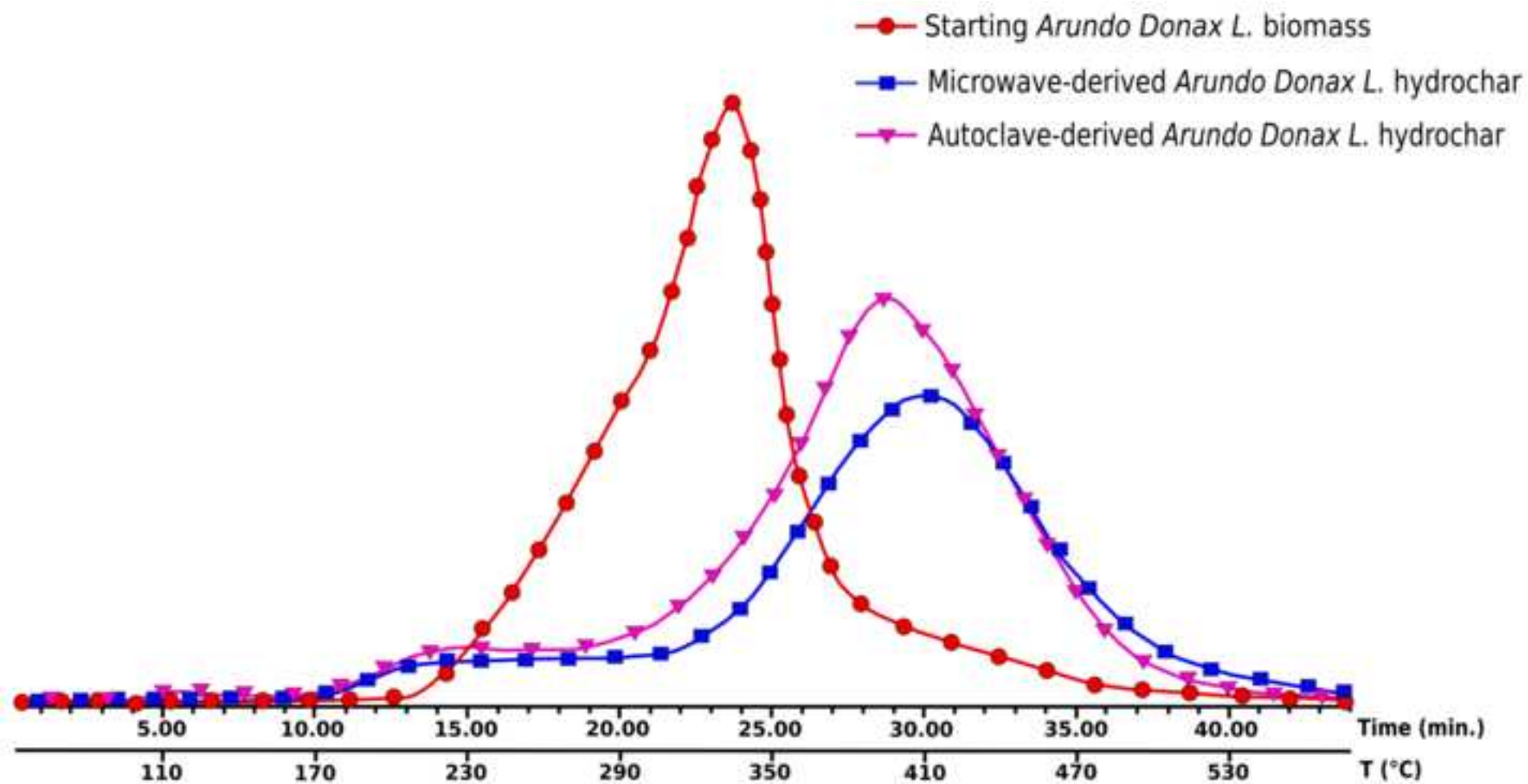


Figure 4

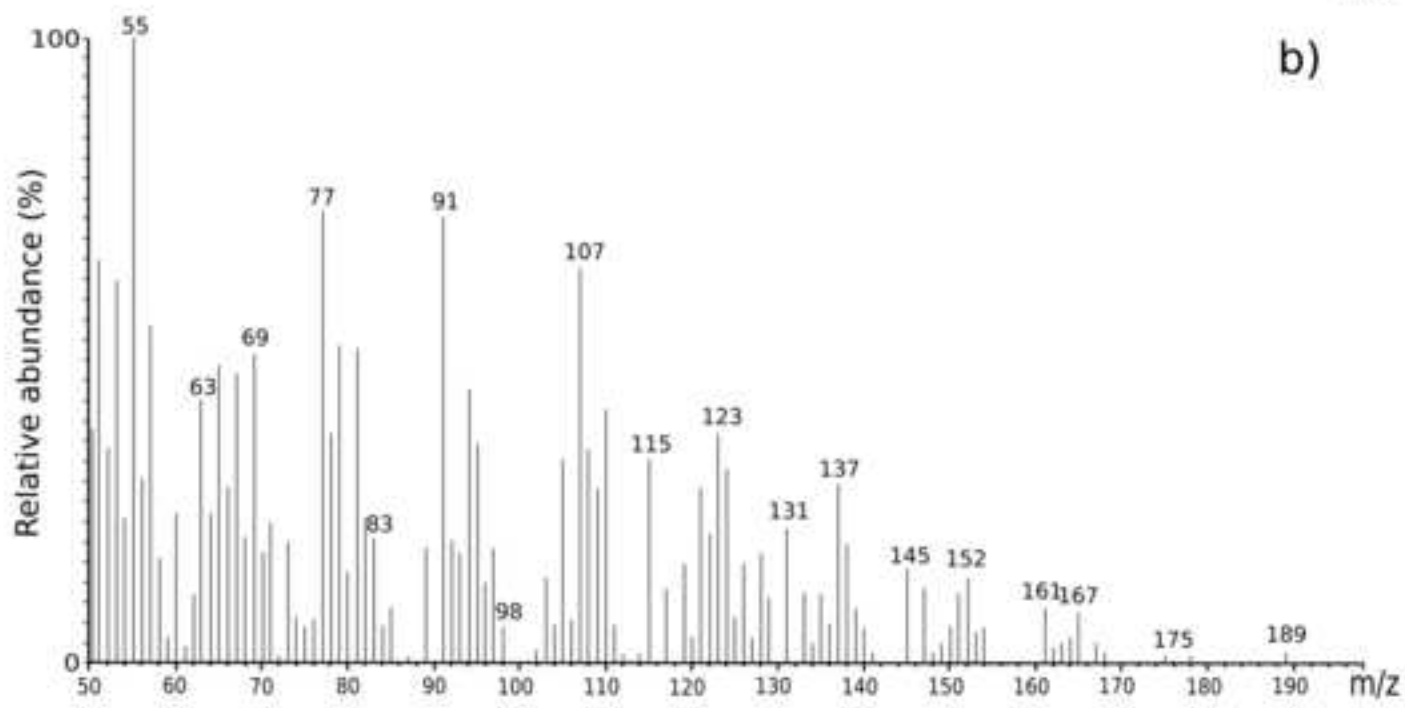
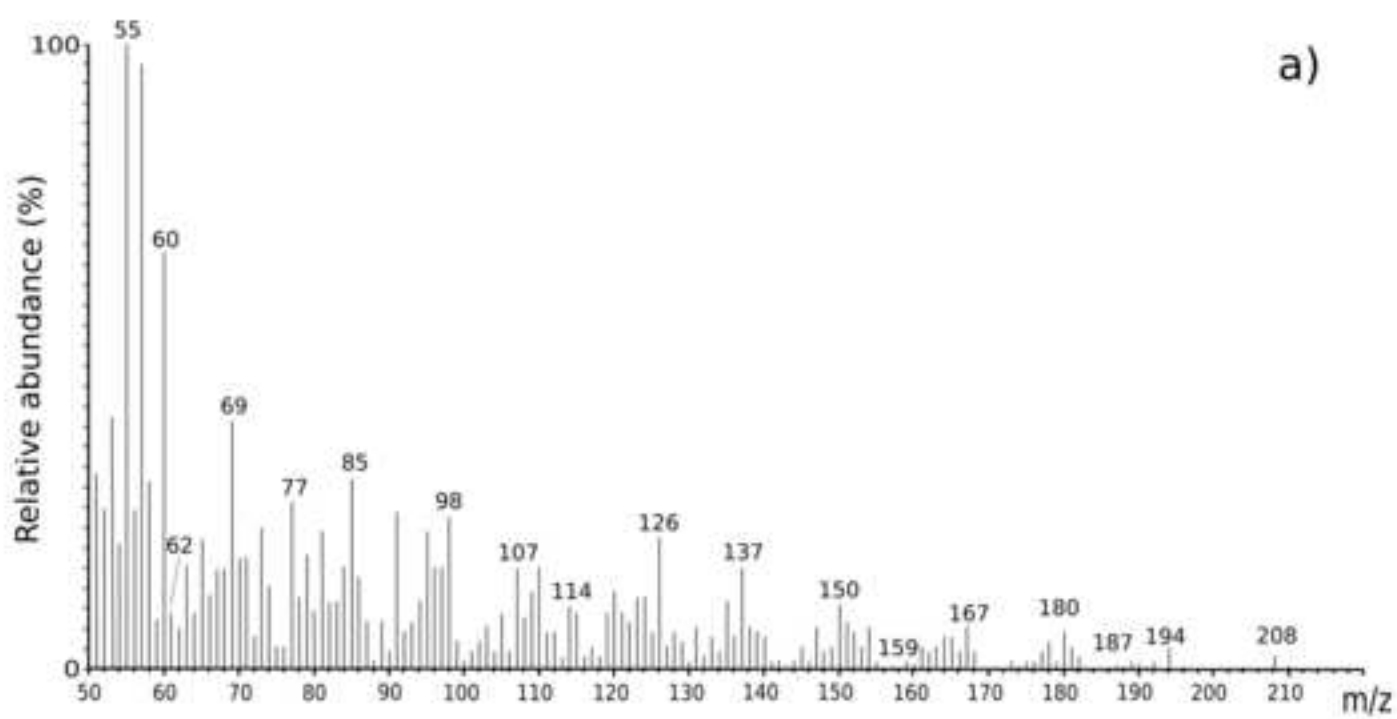


Figure 5

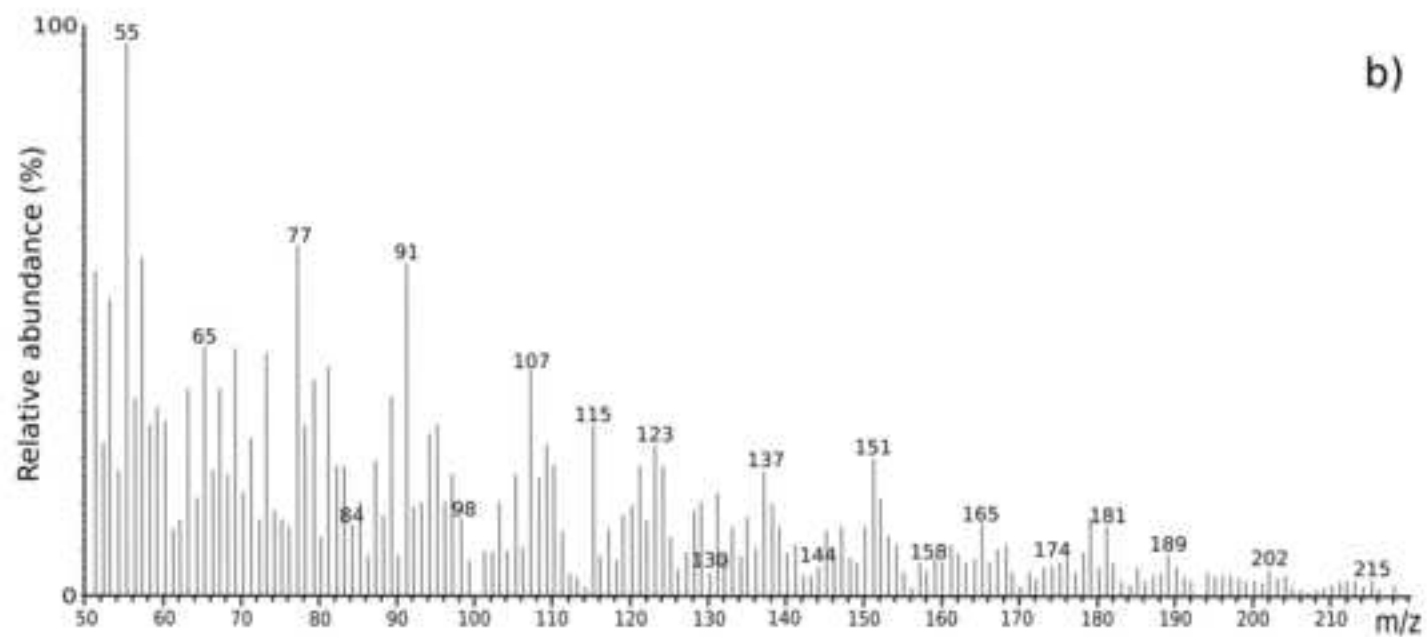
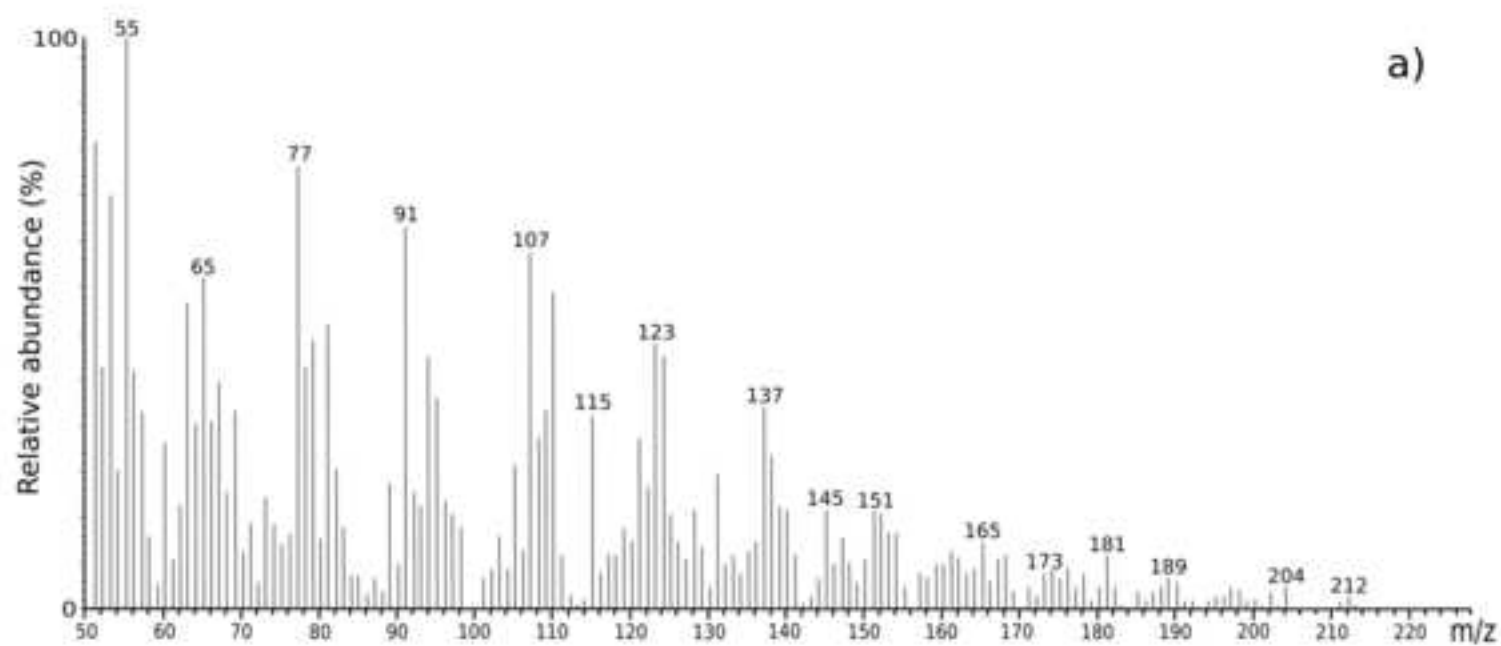


Figure 6

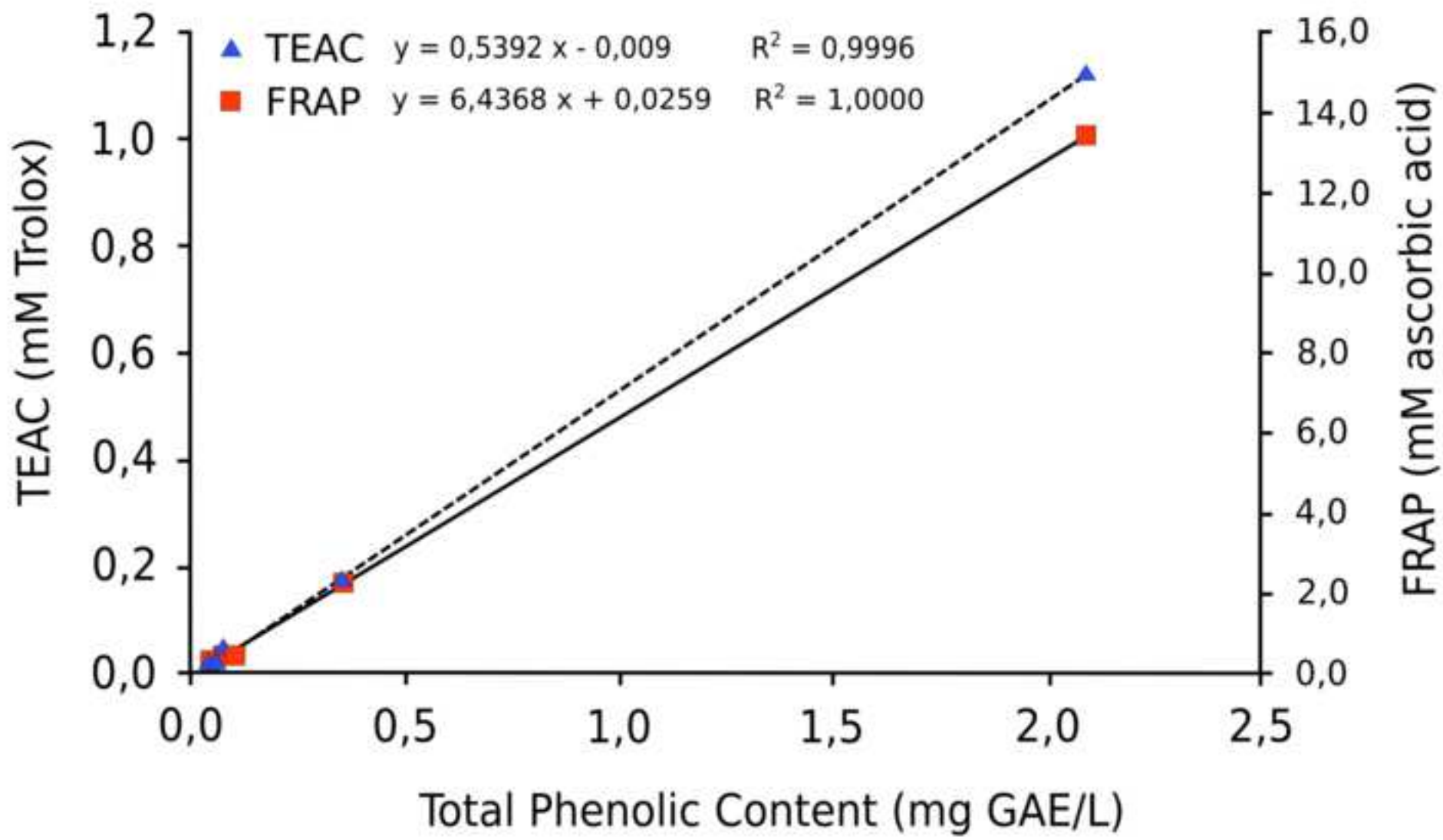
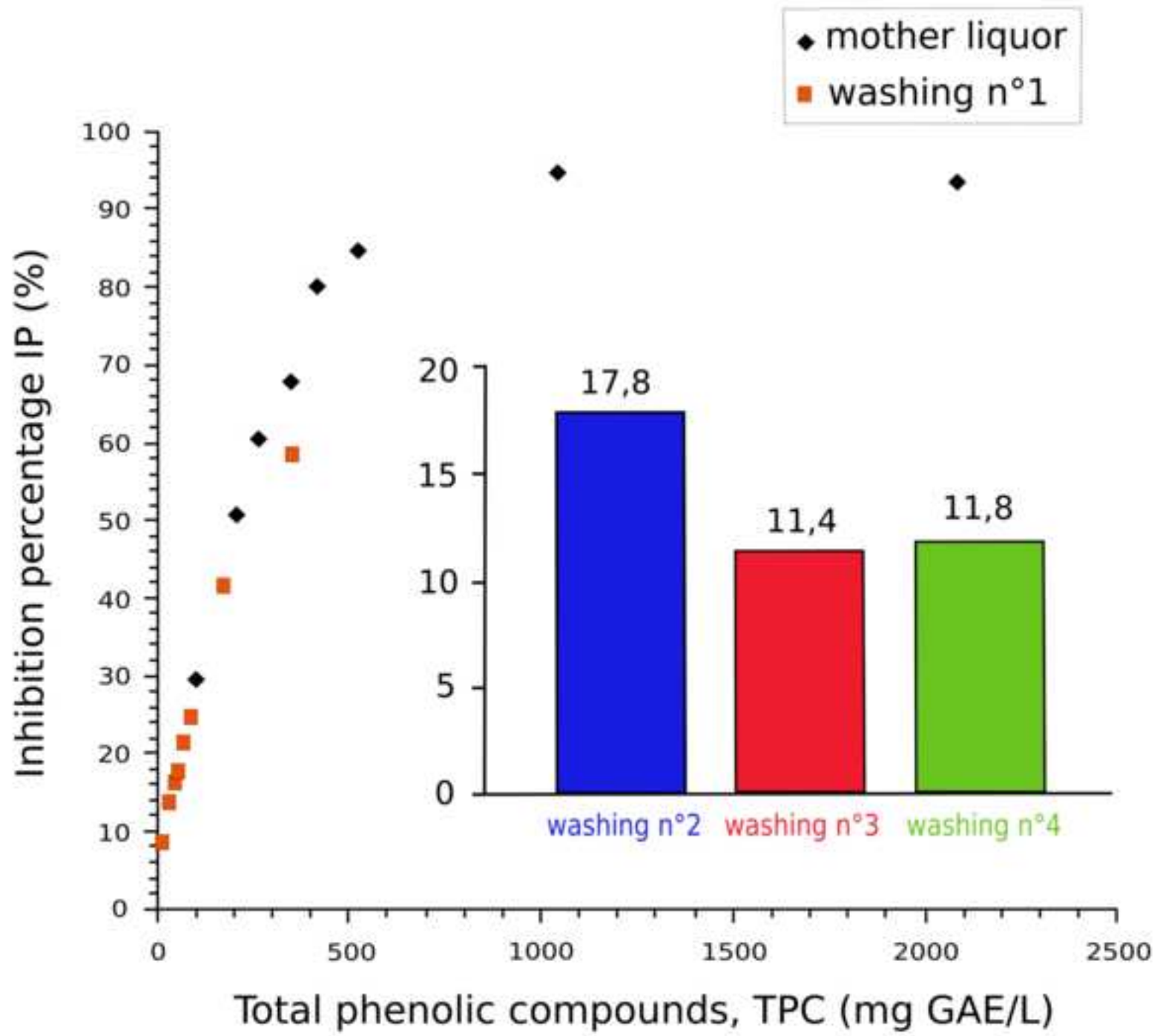


Figure 7



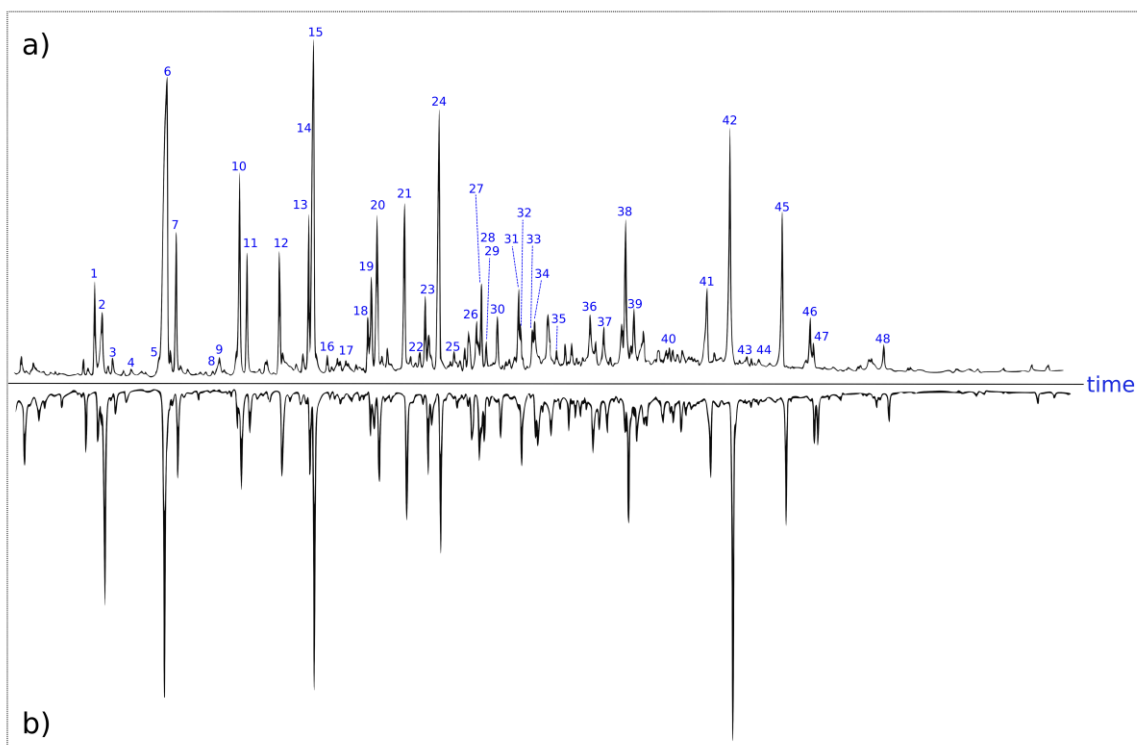


Fig. S1 Pyrograms of (a) microwave- and (b) autoclave- derived *Arundo Donax* L. hydrochars, under the best reaction conditions for LA synthesis. The identification of the numbered peaks is reported in Table 2.

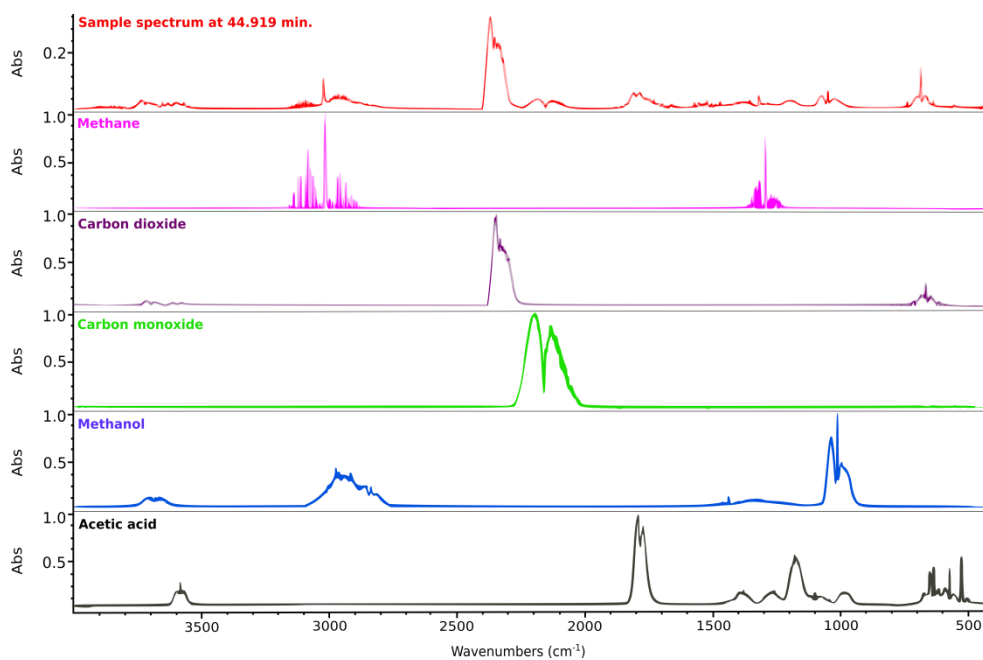


Fig. S2 Comparison of the FTIR spectrum of the gas deriving from autoclave- derived hydrochar pyrolysis in TGA at 400 °C and those of the best-matched compounds, on the basis of the available electronic libraries.

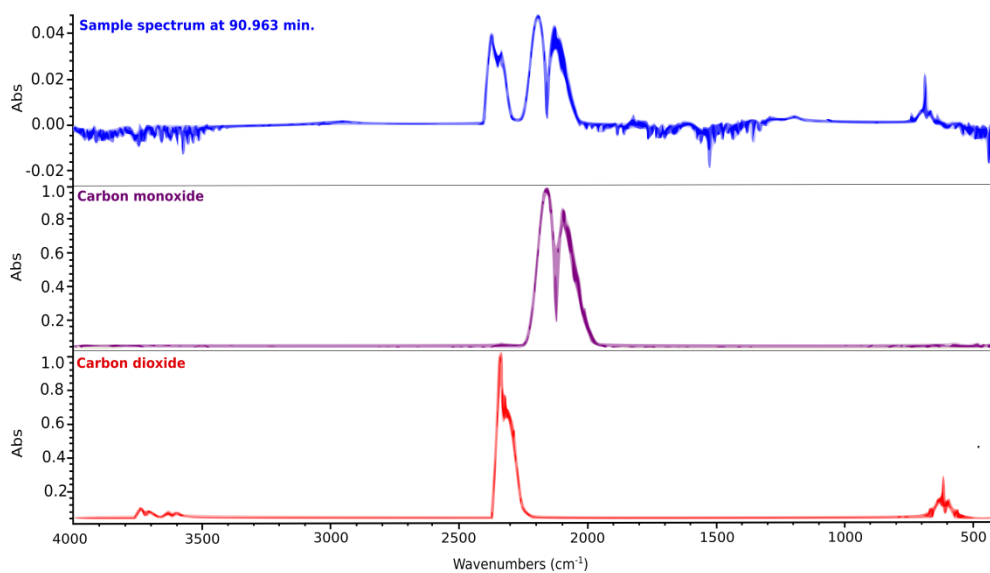


Fig. S3 Comparison of the FTIR spectrum of the gas deriving from autoclave- derived hydrochar pyrolysis in TGA at 850 °C and those of the best-matched compounds, on the basis of the available electronic libraries.

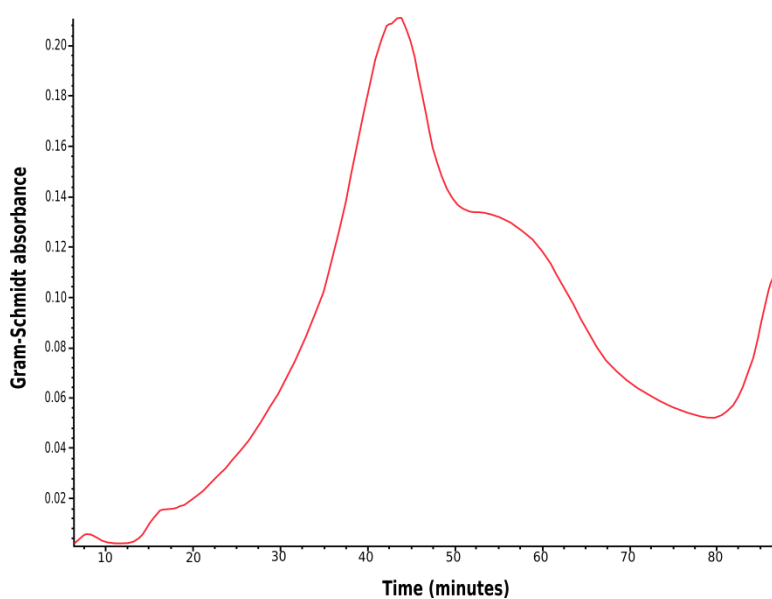


Fig. S4 Gram-Schmidt plot of the gas evolved from the autoclave-derived *Arundo Donax* L. hydrochar.

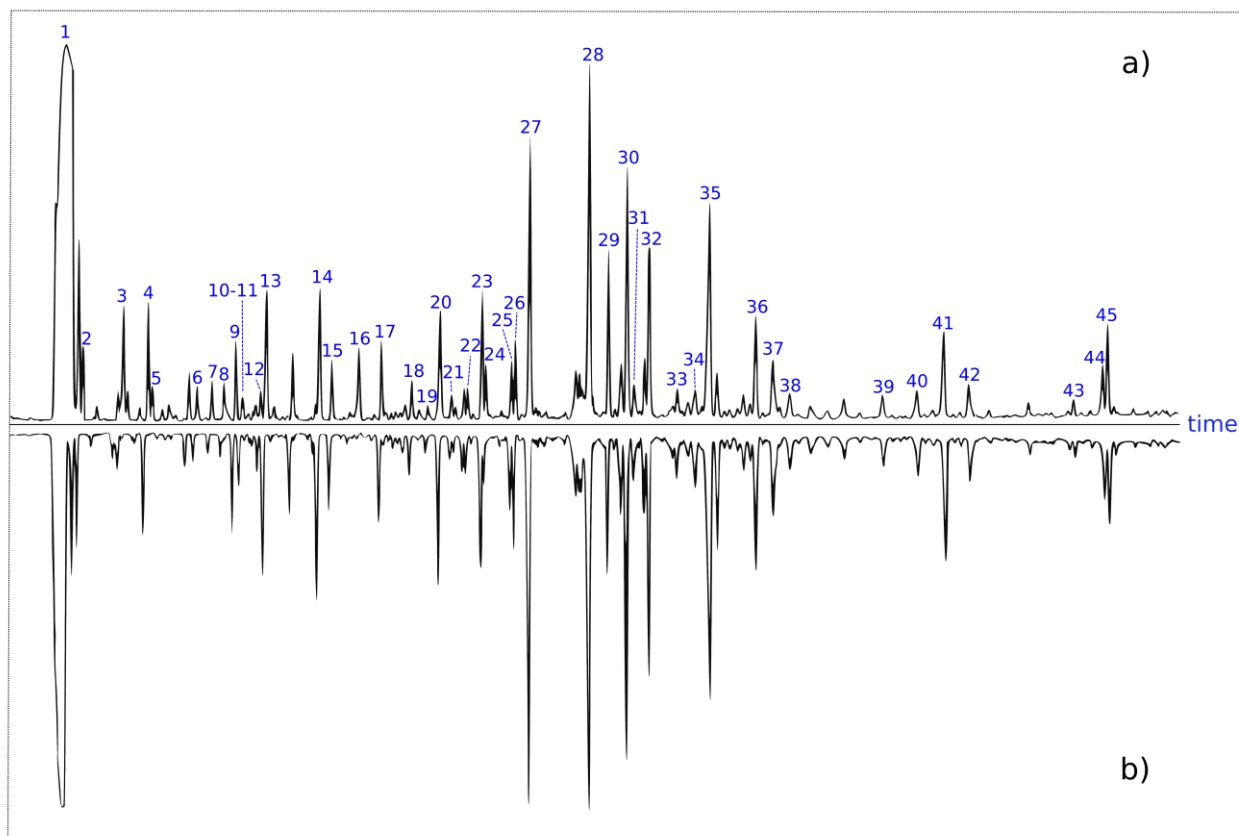


Fig. S5 GC/MS chromatograms of the mother liquors recovered after *Arundo Donax* L. hydrolysis in **(a)** microwave and **(b)** autoclave systems, under the best reaction conditions to give LA. The corresponding assignments are reported in Table 3.